

ACID FRACTURE AND FRACTURE CONDUCTIVITY STUDY ON  
HETEROGENEOUS CARBONATE ROCK SAMPLES

A Thesis

by

XICHEN WANG

Submitted to the Office of Graduate and Professional Studies of  
Texas A&M University  
in partial fulfillment of the requirements for the degree of  
MASTER OF SCIENCE

Chair of Committee,	Ding Zhu
Committee Members,	A. Daniel Hill Yuefeng Sun
Head of Department,	A. Daniel Hill

December 2015

Major Subject: Petroleum Engineering

Copyright 2015 Xichen Wang

## ABSTRACT

Acid fracturing is a widely used stimulation technique for carbonate reservoirs, and more efficient both technically and economically compared with propped fracturing. However, the performance of acid fracturing is hard to predict, and the technique does not always provide sufficient improvement to the productivity. Furthermore, it is even more challenging to stimulate deep wells in heterogeneous reservoirs with high temperature and pressure environments. In this study, experiments were conducted on field cores to investigate the influence of rock lithology, permeability, porosity on fracture conductivities.

Five carbonate core samples from three different wells were tested. All samples are composed of limestone and dolomite with different compositions. The permeability varies within the range of 0.002 md to 0.006 md and the porosity ranges from 1.6% to 3.0%. To compare the results, unpropped and propped hydraulic fracture conductivity tests were also performed on all five core samples along with acid fracture conductivity tests. Experimental conditions, such as acid type, injection rate, contact time, system temperature, and leak-off acid volume were recorded during the acid etching tests. Additionally, the fracture surfaces of each sample were scanned before and after the acid treatment to calculate the total acid etched volume and to characterize the changes in surface profiles.

The results indicated that the formation characteristics had a significant influence on the acid fracture conductivity. The sample with mainly dolomite was less reactive to

acid and had less acid etching volume than the samples with mainly limestone.

Furthermore, the heterogeneity of the sample rock had a direct impact on the roughness of the fracture surface, which also affected acid etching pattern, acid leak-of volume, and acid fracture conductivity results.

## DEDICATION

To my mother and my lifelong friends Alan V. Truong and Ryan X. Ji.

## ACKNOWLEDGEMENTS

I would like to thank Dr. Zhu for giving me the opportunity to research in the acid fracture group. She not only taught me how to become a good researcher and engineer, but also helped me to overcome a huge obstacle in my life.

I would like to thank Dr. Hill for serving on my committee and offering wisdom and experience to my research.

I would also like to thank Dr. Sun, for serving on my committee and guidance and support throughout the course of this research.

Thanks also go to my friends and colleagues Jarrod Underwood and Assiya Suleimenova for sharing their experiences on their research and making my time at Texas A&M University a great experience.

Finally, thanks to my mother and father for their encouragement and unconditional love.

## NOMENCLATURE

$\rho$	density, lb/ft <sup>3</sup> or kg/m <sup>3</sup>
$\mu$	viscosity, cP or Pa-s
$v$	fracture flow velocity of the in the, ft/s
$w$	fracture width, in
$(p_1^2 - p_2^2)$	pressure squared difference across the fracture, psi <sup>2</sup>
$k_f w$	fracture conductivity, md-ft
$q$	flow rate, liter/s
$M$	molecular mass, kg/kg-mol
$h$	height of fracture face, in
$Z$	compressibility factor
$R$	universal gas constant, J/mol-K
$T$	temperature, K
$L$	length of fracture, in
$x_f$	fracture half length, ft
$C_{fD}$	dimensionless conductivity
$r_w$	wellbore radius, ft
$r_w'$	effective wellbore radius, ft
$S_f$	equivalent skin effect
$J_{Dpss}$	dimensionless pseudosteady-state productivity index
$S_c$	choke skin
$J_{DTH}$	dimensionless productivity index for a transverse fracture

## TABLE OF CONTENTS

	Page
ABSTRACT .....	ii
DEDICATION .....	iv
ACKNOWLEDGEMENTS .....	v
NOMENCLATURE .....	vi
TABLE OF CONTENTS .....	vii
LIST OF FIGURES .....	ix
LIST OF TABLES .....	xi
CHAPTER I INTRODUCTION AND LITERATURE REVIEW .....	1
1.1 Introduction .....	1
1.2 Literature review .....	3
1.2.1 Factors that affect the performance of acid fracture treatment .....	3
1.2.2 Experimental studies on acid fracture conductivity .....	5
1.3 Research objective.....	8
CHAPTER II EXPERIMENTAL APPARATUS AND PROCEDURES .....	9
2.1 Experimental apparatus .....	9
2.1.1 Acid etching apparatus .....	9
2.1.2 Fracture conductivity measurement apparatus .....	13
2.1.3 Surface characterization apparatus .....	14
2.2 Experimental procedures and calculations .....	16
2.2.1 Core sample preparation.....	17
2.2.2 Acid etching test procedures .....	20
2.2.3 Conductivity measurement procedures and calculation .....	23
2.2.4 Fracture surface characterization.....	30
CHAPTER III EXPERIMENTAL RESULTS AND DISCUSSION .....	32
3.1 Field sample description.....	32
3.2 Acid etching test results .....	34
3.2.1 Well 1 sample acid etching test results .....	34

3.2.2 Well 2 samples acid etching test results .....	36
3.2.3 Well 3 sample acid etching test results .....	38
3.3 Fracture conductivity test results.....	40
3.3.1 Well 1 sample fracture conductivity test results .....	40
3.3.2 Well 2 sample fracture conductivity test results .....	43
3.3.3 Well 3 samples fracture conductivity test results .....	47
3.3.4 Conductivity measurement comparisons of three wells.....	50
3.4 Productivity calculation results .....	54
 CHAPTER IV CONCLUSIONS AND RECOMMENDATIONS .....	 58
4.1 Conclusions .....	58
4.2 Recommendations .....	59
 REFERENCES .....	 60
 APPENDIX A .....	 64
 APPENDIX B .....	 67
 APPENDIX C .....	 73



## LIST OF FIGURES

	Page
Figure 1. The processes of acid fracturing (Pounik 2008) .....	1
Figure 2. Dynamic acid etching test apparatus diagram .....	9
Figure 3. The image of modified API conductivity cell (a); O-ring slot inside of conductivity cell (b) and O-ring slot on the piston(c).....	11
Figure 4. Fracture conductivity measurement test apparatus diagram.....	13
Figure 5. The image of the surface laser profilometer .....	15
Figure 6. The flow chart of the experimental procedures .....	17
Figure 7. The images of core sample before (left) and after (right) sample preparation .	18
Figure 8. The images of three stages rock preparation .....	20
Figure 9. The image of prepared sample for acid etching test .....	20
Figure 10. The image of water saturation apparatus .....	21
Figure 11. The image of core sample before (left) and after (right) acid etching test .....	23
Figure 12. The image of prepared sample for propped conductivity test.....	24
Figure 13. Prepared core sample for conductivity test.....	24
Figure 14. An example plot to calculate fracture conductivity .....	30
Figure 15. An example of surface profile generated by Matlab.....	31
Figure 16. Tarim basin location map (Knusser, 2008).....	33
Figure 17. The images of sample A surface profile changes before and after acid etching.....	35
Figure 18. The images of sample B surface profile changes before and after acid etching.....	36
Figure 19. The images of sample C surface profile changes before and after acid etching.....	37

Figure 20. The images of sample D surface profile changes before and after acid etching.....	38
Figure 21. Sample A fracture conductivity data at different closure stress for acid fracture experiment along with unpropped and propped experiments .....	42
Figure 22. Sample B and C fracture conductivity data at different closure stress for acid fracture experiment along with unpropped and propped experiments.....	46
Figure 23. Sample D and E fracture conductivity data at different closure stress for acid fracture experiment along with unpropped and propped experiments.....	49
Figure 24. The effect of rough surface on fluid flow .....	50
Figure 25. Sample A-E fracture conductivity data at different closure stress for propped fracturing experiments .....	52
Figure 26. Sample A-E fracture conductivity data at different closure stress for propped fracturing experiments .....	54

## LIST OF TABLES

	Page
Table 1. Fracture conductivity calculation parameters .....	28
Table 2. An example sheet to calculate fracture conductivity .....	29
Table 3. Formation characteristics of investigated well.....	33
Table 4. Rock properties of the tested samples .....	34
Table 5. The volumes of the dissolved rock.....	39
Table 6. The experimental condition of conductivity tests on sample A .....	41
Table 7. The experimental condition of conductivity tests on sample B .....	45
Table 8. The experimental condition of conductivity tests on sample C .....	45
Table 9. The experimental condition of conductivity tests on sample D .....	48
Table 10. The experimental condition of conductivity tests on sample E .....	48
Table 11. Calculated post-fracture productivity index .....	57

## CHAPTER I

### INTRODUCTION AND LITERATURE REVIEW

#### 1.1 Introduction

Acid fracturing technique is widely used in carbonate reservoir stimulation, and it is easier and cheaper to apply compare with propped fracturing. The purpose of acid fracturing treatment is to create conductive fractures in the formation by using acid and other material. The treatment can enhance the oil and gas production or water injection.

In acid treatments, viscous pad fluid is first injected into the formation to initiate a hydraulic fracture. Then, acid is injected at pressures higher than rock fracturing pressure to further propagates the fracture, meanwhile, acid reacts with the fracture walls and creates uneven surfaces. The unevenness of fracture surfaces could possibly result in a conductive pathway. **Figure 1** shows the processes of acid fracturing.

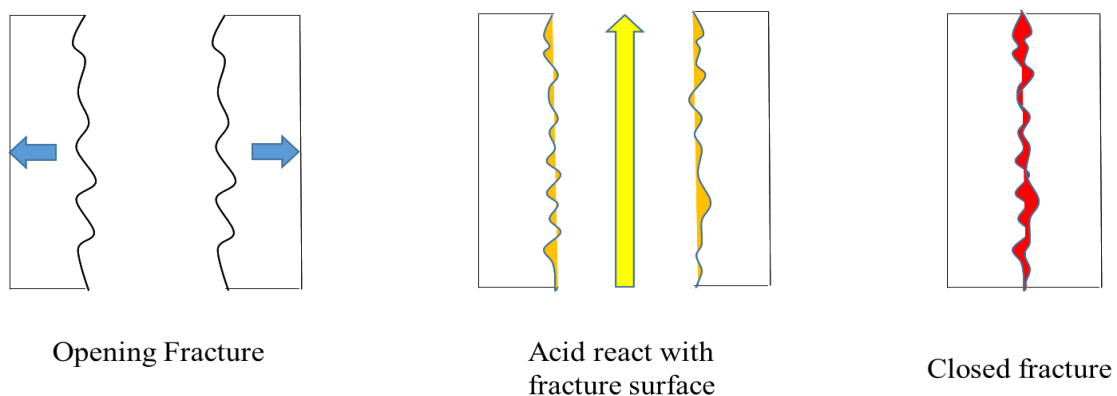
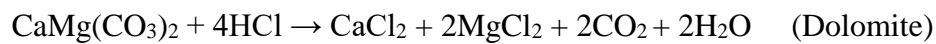
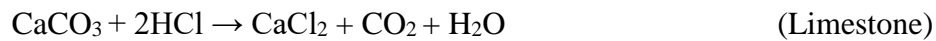


**Figure 1.** The processes of acid fracturing (Pounik 2008)

Hydrochloric acid (HCl) is commonly used for carbonate formation stimulation. The type of acid fracture fluid mixtures, for example plain acid, gelled acid, foamed acid, or emulsified acid are all used in carbonate acidizing (Mirza et al. 1996). Carbonate formation is mainly composed of limestone and dolomite. The chemical reactions between HCl and limestone or dolomite are given by



Acid fracturing is an economical well stimulation technique. However, acid treatments cannot always provide sufficient conductivity due to the stochastic nature of acid reaction with carbonate formations.

To theoretically is extremely challenge due to the lack of understanding about the reservoir properties, especially permeability and mineralogy distribution. Various parameters affect the performance of acid fracturing treatments. Such parameters including rock properties, reservoir characteristics and treatment conditions. Currently, the most common and practical way to design an acid fracturing treatment is direct laboratory experiments on the core samples from the target formation to determine the appropriate treatment conditions.

This research is aimed to evaluate the factors that affected the efficiency of acid fracturing for heterogeneous carbonate formations. Experiments were conducted on field core samples to determine the fracture conductivity at reservoir condition, and identify the conditions that yield more effective stimulation. To evaluate which stimulation

method should be used, acid fracturing test results were also compared with hydraulic fracturing test results.

## **1.2 Literature review**

### *1.2.1 Factors that affect the performance of acid fracture treatment*

Commonly used method for acid fracture prediction is an empirical correlations developed by Nierode and Kruk (1973). The predictions involved rock mechanical strength and dissolved rock equivalent conductivity. The correlations uses an average fracture width that is estimated from the volume of dissolved rock when assume a rectangular shaped fracture face with constant fracture height and width. The corresponding fracture conductivity associated with the channel was defined as dissolved rock equivalent conductivity (DREC). In addition, the rock embedment strength (RES) and applied closure stress were also considered in Nierode and Kruk model.

Anderson and Fredrickson (1989) summarized that the quantity of removed rock and the pattern of rock were the two primary factors influencing the resultant fracture conductivity. Kinetic parameters such as acid type and strength, reaction temperature, reaction time, and flow regime affect the amount of rock removed during the acidizing process. They also indicated that formation characteristics have the dominate effect on acid fracture conductivity. The mineralogical composition of the formation have a direct influence on the degree of heterogeneity in the fracture face. Therefore, the degree of heterogeneity affect the acid etching pattern.

Navarrete et al (1998) explained two characteristics of fracture formed by acid reaction: length of a conductive fractures and conductivity of the fracture. The competition between acid fluid loss and acid reaction rate with the formation determines the acid flow rate along the fracture. Furthermore, Zou et al (2005) pointed out that acid fracture performance varies significantly with acid fluid type, pumping schedule, formation composition, rock embedment strength, reservoir pressure, and other downhole conditions.

Mou (2009) showed in their study that channeling type of acid fracturing in heterogeneous reservoir has been ignored in typical fracturing simulations and could not be captured in small scale laboratory measurement. Therefore, they developed an intermediate-scale acid fracture model with grid size small enough, but the domain dimension big enough to capture local and macro heterogeneity effects and channeling characteristics. Their test reports shown that channels extending from the inlet to the outlet of the fracture creates high and sustainable conductivity, since channels are hard to crush and conductivity can be maintained after closure.

Deng et al (2012) introduced a new approach to acid fracture modeling. The approach used intermediate scale to simulate acid transport, acid dissolution, and rock elastic deformation under closure stress. The purpose of this simulation is to fill the gap between laboratory measurement and macro scale acid fracture models. They concluded that the permeability distribution of the formation affects the closure behavior of an acid fracture. Also, according to their study, the correlation developed by Nierode and Kruk does not predict conductivity correctly when channels are formed.

Oeth (2013) developed a fully three-dimensional model to evaluate and predict acid fracturing performance. The model can solve the three dimensional equations that describes acid transport and reaction within a fracture, it can also predict the etched width that created by acid along the fracture. The most important feature of this model is that the fracture interiors is gridded in all three directions. The model captures the fundamentals of acid fracturing process much more accurately.

In conclusion, the industry lack of quantitative method to evaluate an acid fracture treatment. The laboratory experiment using formation samples and same fluid system planned for fracturing treatment still is the best way to evaluate a fracturing treatment.

### *1.2.2 Experimental studies on acid fracture conductivity*

Anderson and Fredrickson (1989) developed an experimental study to measure core sample acid fracturing conductivity. Their test results proved that fracture conductivity were affected by acid type, acid concentration, reaction time, temperature, flow regime and the amount of rock dissolved.

Beg et al (1998) conducted a series of experiments to measure core sample acid fracture conductivity as a function of closure stress. They concluded that over-etching the fracture surface caused the conductivity decrease. Also, acid leak-off can sometimes help to increase the fracture conductivity. They also found that Nierode-Kruk correlation gave better predictions if the acid that flows into the formation was not included. Furthermore, they observed that deep channels, which created on the surface of a fracture, result in high fracture conductivities.



Gong et al (1998) performed a systematic experimental study to investigate the mechanisms of creation of hydraulic conductivity in acid fracturing, including characterization of surface roughness created by acid etching, investigation of damage to the rock compressive strength by acid, and measurement of hydraulic conductivity under closure stress. The experimental data showed that longer acid contact results in rougher fracture surfaces and, in turn, higher hydraulic conductivity. However, acidizing also reduces the rock compressive strength causing the surface asperities to easily deform under stress.

Malagon et al (2006) measured fracture surface etching profiles for a wide range of acidizing conditions. The measurement result showed that the etched surface characteristics depended on acidizing condition, including acid type, strength, velocity in the fracture, leak-off rate and rock type.

Melendez (2007) studied the effects of hardness variation and surface etching on acid fracture conductivity. The experimental results proved that acid-etched surface channels dominate the conductivity after closure, whereas rock strength dominate the conductivity in the cases of no acid-etched channels were created. The study tested three carbonate rocks; Texas Cream chalk, Indiana limestone and San Andrea dolomite. Texas Cream chalk samples had the lowest rock strength values and the fractures closed at much lower stress compared with the limestone and dolomite samples, which had higher hardness values. Furthermore, the San Andrea dolomite samples had the highest rock embedment strength and best conductivity results compared with other rocks tested. The dolomite samples retained conductivity at high closure stress even without channels.

Pournik et al (2007) conducted a series of laboratory tests that mimic the conditions in actual field acid fracture treatment. Their test results indicated that longer acid contact time did not create larger fracture conductivities. Additionally, the acid fracture conductivities measured in their lab do not agree with the predictions from the Nierode-Kruk correlation.

Neumann et al (2012) tested the feasibility of acid fracturing on hard limestone rocks from deep formation. They conclude that acid fracture conductivity can retain under closure stress greater than 5000 psi. Moreover, they used the linear roughness parameter to characterize fracture surfaces. Acid fracturing conductivity window was introduced to determine the feasibility in their study.

Another study done by Neumann et al (2012) discussed the different effect of asperities paradigm on rocks with wet sawed fracture surfaces and rocks with tensile fracture surfaces. In this study, they use both linear roughness and tensile linear roughness to characterize fracture surfaces.

Almomen et al (2013) conducted an experimental study to determine the effects of acid fracturing treatment variables on fracture conductivity. They scaled down the field treatment conditions to laboratory scale by matching Reynold's and Pelect numbers. The results showed that rough surface fractures generate higher conductivity than smooth surface fractures did. Also, acid etched volume is not adequate to predict the conductivity.

### **1.3 Research objective**

The main objective of this study is to evaluate the factors that affect the efficiency of acid fracturing for heterogeneous carbonate formation. Experiments were designed with the field core samples to test the parameters that were important for evaluating acid fracture treatments. Five core samples were tested under the conditions that scaled down from real field treatment. Samples were tested for acid fracture conductivities under different closure stresses, along with unpropped and propped hydraulic fracture conductivities as references.

## CHAPTER II

### EXPERIMENTAL APPARATUS AND PROCEDURES

#### 2.1 Experimental apparatus

Three major apparatus were used in this experimental study, including the acid etching apparatus, the fracture conductivity measurement apparatus, and the surface characterization apparatus.

##### 2.1.1 Acid etching apparatus

Acid etching apparatus consisted of a modified conductivity cell, a high volume pump, three pressure transducers, two backpressure regulators, and a heating system.

The experimental apparatus of acid etching test was shown in **Figure 2**.

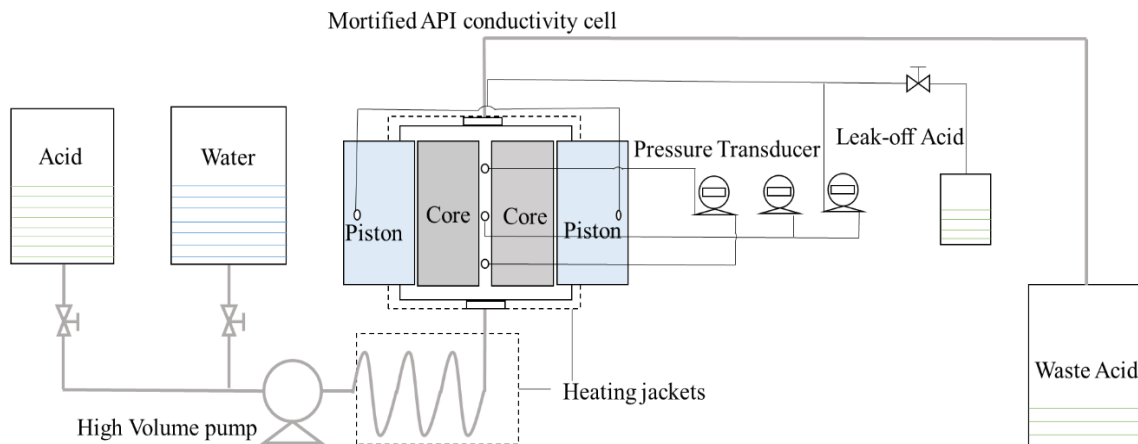
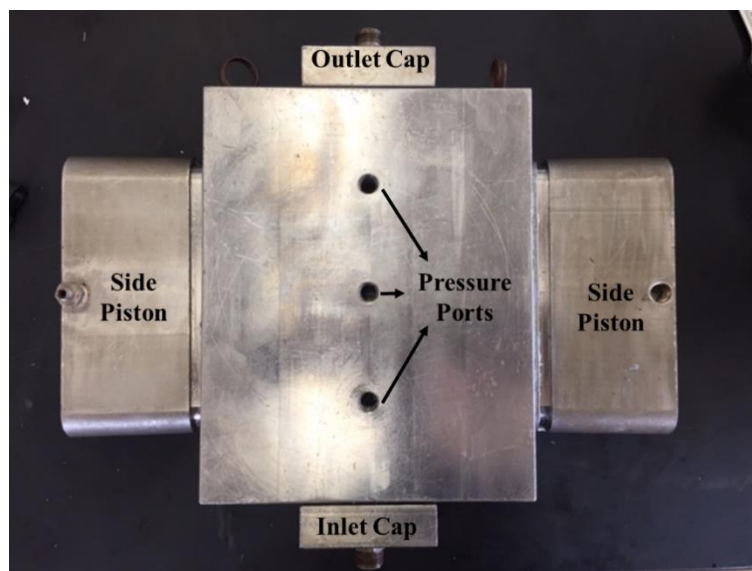
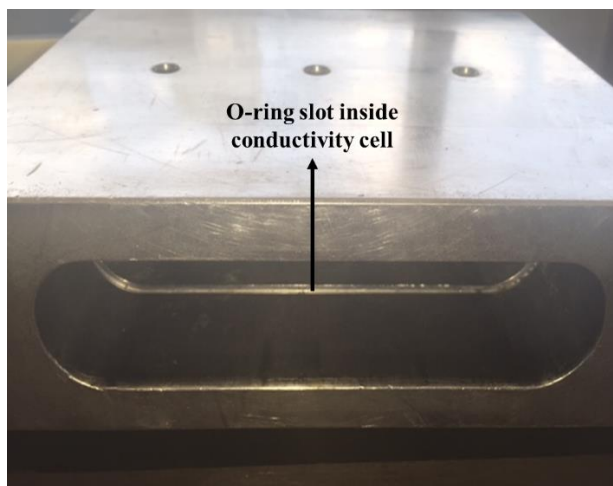


**Figure 2.** Dynamic acid etching test apparatus diagram

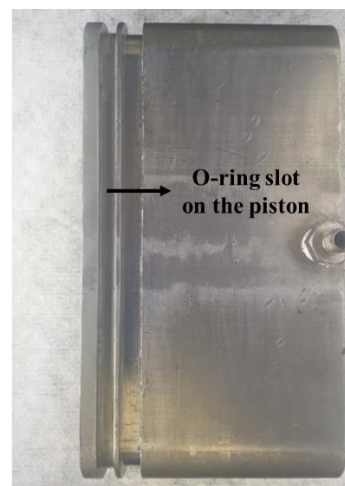
A modified API conductivity cell was used to hold the core sample in place during the acid etching test. To ensure CO<sub>2</sub> that was produced from acid reaction stays dissolved in the solution, the cell pressure was set to 1000 psi using a backpressure regulator. The conductivity cell was made of hastelloy in order to resist corrosion and to hold up the pressure of experimental condition. The outer dimensions of the conductivity cell were 10-in. long, 3-1/4-in. wide and 8-in thick. Whereas, the interior space were able to hold rock samples with 7.11-in. long, 1.61-in wide and 6-in thick. Two slots that located inside of the cell were used for placing O-rings to seal off the cell pressure. Core sample were pushed into the cell with a hydraulic jack after O-rings were glued into the slots. Three pressure ports in the middle of the cell were designed to connect pressure transducers. Two side pistons were pushed into the cell after the samples were in place. The pistons also had slots on them for placing O-rings to prevent fluid and pressure leakage. **Figure 3** displayed the setting of the assembled conductivity cell (a); O-ring slot inside of conductivity cell (b) and O-ring slot on the piston (c).



(a)



(b)



(c)

**Figure 3.** The image of modified API conductivity cell (a); O-ring slot inside of conductivity cell (b) and O-ring slot on the piston(c).

Three pressure transducers were built in the acid etching system. The leak-off pressure transducer, which was connected to the two ports on the side pistons and the

middle point port on the conductivity cell, monitors the acid leak-off differential pressure. Additionally, an outlet within the leak-off flow line was designed to collect the leak-off acid. The cell pressure transducer was only connected to the middle port on the conductivity cell aimed to monitor the absolute cell pressure. The fracture differential pressure transducer, which connected to the top and bottom ports on the conductivity cell, monitors the differential pressure along the fracture. The fracture differential pressure transducer and leak-off differential pressure transducer had a maximum pressure rate of 30 psi. The cell pressure was measured by a transducer with a maximum pressure rate of 1500 psi.

A high volume pump used in acid etching test has a maximum pump rate of 1.05 liters/minutes. 1 liter/minutes pump rate upscale to 20 barrels/minute in field condition (Pournik, 2007).

Two backpressure regulators were connected to the flow line in order to achieve a cell pressure of 1000 psi and a leak-off pressure of 20 psi. The purposes of applying the backpressure were: 1) to keep CO<sub>2</sub> generated from acid reaction to stay dissolving in the solution; 2) to create a differential pressure across the fracture about 20 psi.

The heating system included two heating jacket and two thermocouples. A part of the upstream line was covered by one jacket. Another heating jacket was used to wrap the whole conductivity cell. A thermocouple, connected to the inlet flow line, monitors the injection fluid temperature, while another thermocouple, connected to the jacket on the conductivity cell, monitors the cell temperature.

### 2.1.2 Fracture conductivity measurement apparatus

The fracture conductivity measurement apparatus consisted of a nitrogen tank, a gas flow controller, a CT-250 hydraulic load frame, a modified API conductivity cell, three pressure transducers, a needle valve backpressure regulator, and a data acquisition system. The experimental apparatus of fracture conductivity measurement was shown in **Figure 4**.

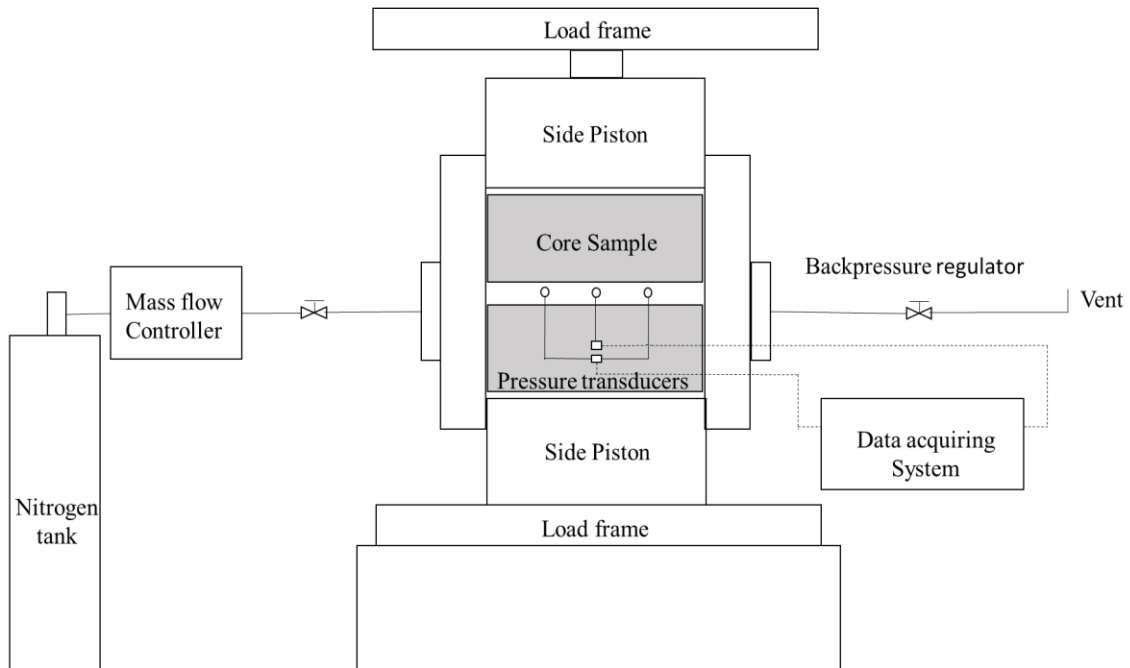


**Figure 4.** Fracture conductivity measurement test apparatus diagram

The nitrogen tank, controlled by a spring valve, provides the conductivity cell the gas flow with a pressure up to 2000 psi. The mass flow controller, connected to the gas



inlet flow line, allowed a maximum flow rate of 10 liters/minute with an accuracy of 0.001 liter/minutes.

The CT-250 hydraulic load frame was used for applying closure pressure on the sample inside the conductivity cell. The maximum stress of the load frame was 16,000 psi (about 875 KN force on a surface area of 12 in<sup>2</sup>). The pressure increases gradually with a rate of 100 psi/minute.

The conductivity cell that used in the conductivity test has the same dimension with the conductivity cell in acid etching test, but it is made of stainless steel instead of hastelloy. Three ports on the conductivity cell connects to two pressure transducers. The two ports on the side were connected to one transducer to measure the differential pressure along the fracture. The third transducer is used to measure the absolute cell pressure through the middle point port. The transducers measured pressures with an accuracy of 0.01 psi.

A needle valve on the outlet flow line functioned as a backpressure regulator. The needle valve together with a spring valve on nitrogen tank, controlled gas flow rate and absolute cell pressure. All the acquired data were shown and recorded in a computer program.

### *2.1.3 Surface characterization apparatus*

Fracture surfaces were scanned before and after acid etching test by a profilometer. The profilometer developed by Malagon (2006) consisted of a laser displacement sensor, two micropulse linear transducers, two stepping-motor units, and a milling table. A Labview program was installed in the computer to process the data.

The laser displacement sensor is AR200-25 from Acuity Laser Measurement Incorporated. It use a triangulation method to measure the distance between the sensor and the object. It has an accuracy of +/- 58.8 $\mu$ m over a range of 25.mm (1in).

The two micropulse liner transducers are used to measure the horizontal displacement through the magnetic wave sensors.

An stepping-motor unit is used to move the milling-table during the measurement. The unit attached to the milling table is a high-torque-low-vibration device. The data from the displacement transducers and the laser sensor are acquired into the Labview software. **Figure 5** was an image of the surface laser profilometer.

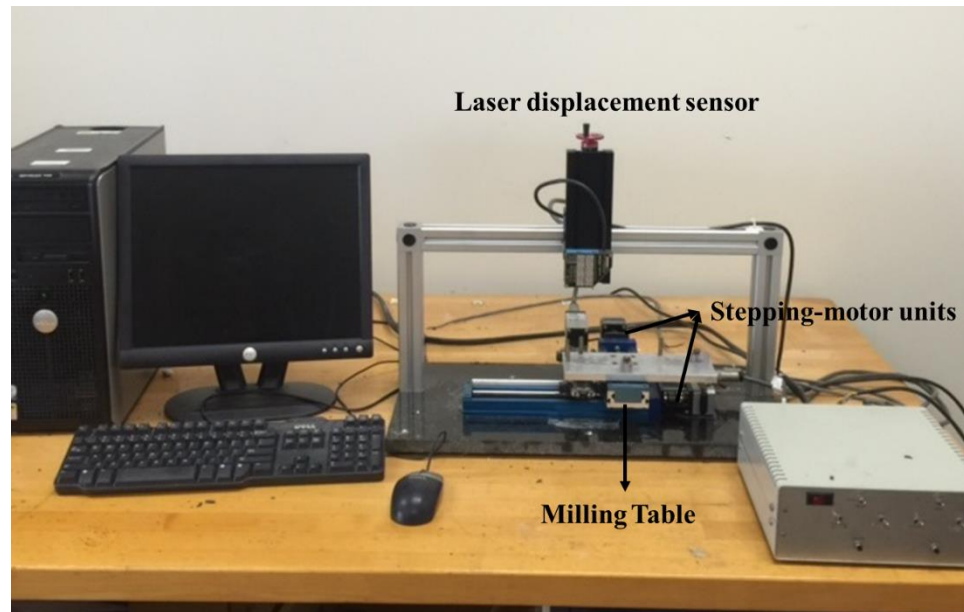


**Figure 5.** The image of the surface laser profilometer

## 2.2 Experimental procedures and calculations

In this study, the rock samples were used three times during a set of test; first, unpropped conductivity test, then propped conductivity test and finally acid fracture conductivity test. First, a sample was prepared for unpropped hydraulic fracture test. After the unpropped hydraulic fracture test, the sample was removed from the conductivity cell carefully to keep the silicon coating in a good condition for the propped conductivity test. The sample was prepared for acid etching test after the propped fracture conductivity test. The acid-etched the sample was prepared again for acid fracture conductivity test. In addition, fracture surface was scanned before and after acid etching test. **Figure 6** is a flow chart that demonstrated the experimental procedures for one core sample.

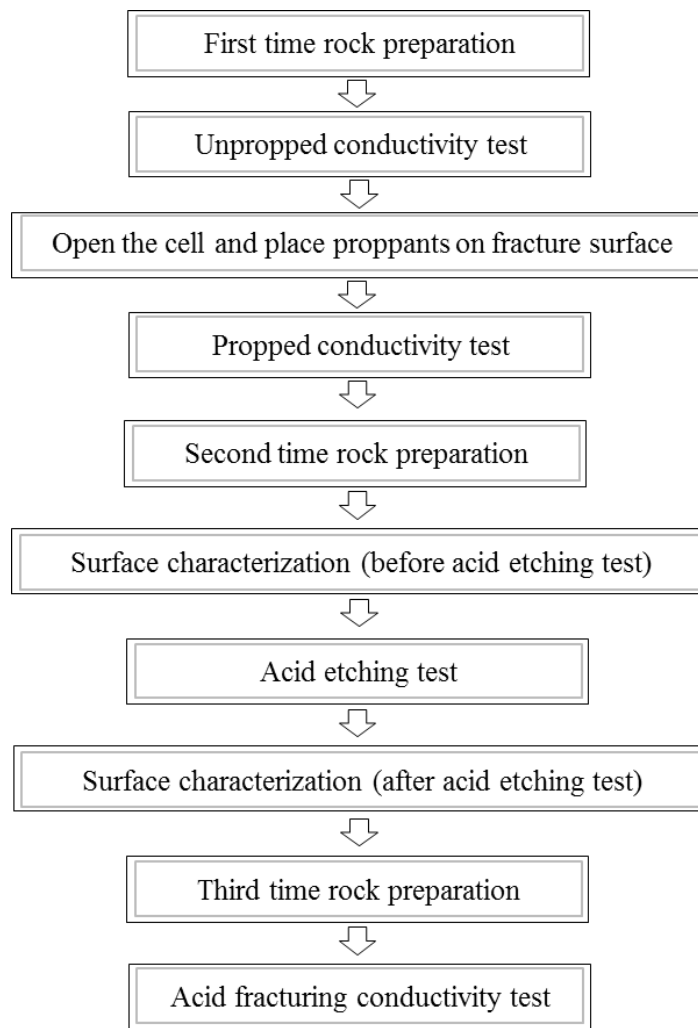


**Figure 6.** The flow chart of the experimental procedures

### 2.2.1 Core sample preparation

All the core samples in this experimental study were less than 3.5 in thick. Since the core samples must meet the required acid injection sample size, the preparation started with gluing the carbonate samples to a sandstone base. The selected sandstone does not have active reaction with HCl acid and has higher permeabilities and porosities than the carbonate samples. The sandstone bases have no influence on the carbonate test

results. After the glue dried up, the sample wall was covered with a layer of silicon in order to perfectly fit into the conductivity cell. **Figure 7** shown the sample before and after sample preparation.

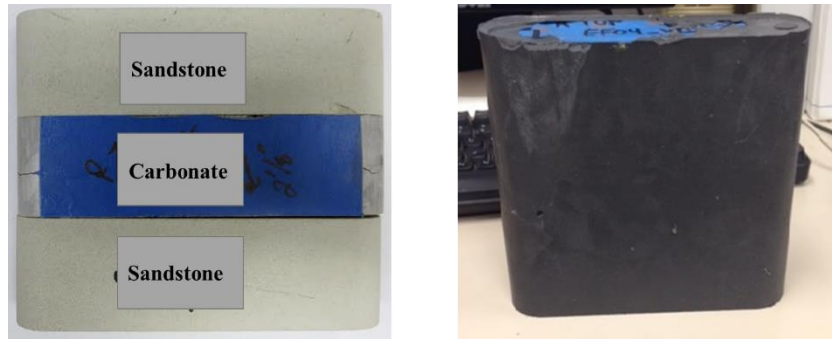


**Figure 7.** The images of core sample before (left) and after (right) sample preparation

Detailed procedures of rock preparation was presented as follow:

- Put the two halves of the sample together after they are well glued to the sandstone base. Use a blue painting tape to cover around the fracture to prevent silicone fluid from entering the fracture.
- Cover the top and bottom of the sample with the blue painting tape to prevent silicone fluid from contaminating the sandstone pores.
- Apply three layer of silicon primer by using a painting brush. Leave 15 minutes in between each application.
- Apply two layer of silicon food (silicon release agent) on the interior wall of the mold.

- Coat the sample with silicon in three stages to avoid generating air bubbles.
- For the first stage, assemble the mold by covering the bottom of the mole with a plastic piece and a metal board to prevent the fluid leakage.
- Place and centralized the sample inside the mold.
- Prepare desired amount of silicon fluid by mixing silicon kit A (color black) and kit B (color white) in the weight ratio of 1:1.
- Pour the silicon fluid into gap between the sample wall and the mold wall until the gap is filled up.
- Leave the sample and mold in the room temperature for an hour to ensure the silicon fluid settling down.
- Move the sample and mold to an oven. Heat the sample for at least 4 hours at the temperature of 60 °C.
- Remove the sample and mold from oven and leave it in room temperature for an hour to cool down.
- Dissemble the mold and remove the sample from the mold.
- For the second stage, tight the mold on the first stage silicon rubber. The rubber serves as a bottom seal for the second stage preparation. Repeat the same steps in the first stage to complete the second stage silicon.
- For the third stage, tight the mold on the second stage silicon rubber. The rubber serves as a bottom seal for the third stage preparation. Repeat the

same steps in the first stage to complete the third stage silicon. **Figure 8** showed the images of three stages rock preparation.

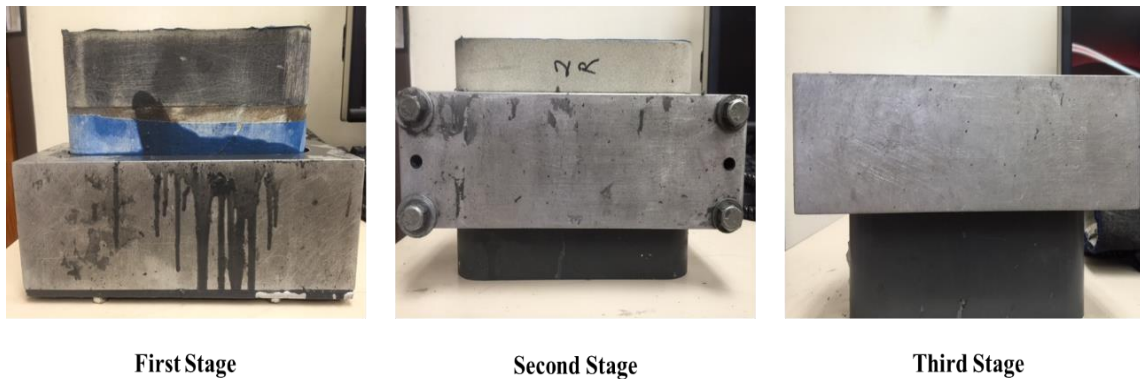


**Figure 8.** The images of three stages rock preparation

### 2.2.2 Acid etching test procedures

For acid etching test, the silicon coat was cut in the middle of the core sample to expose the fracture surface (**Figure 9**).



**Figure 9.** The image of prepared sample for acid etching test

Prepared core samples were fully saturated with water before proceeding to the acid etching test. The core samples were water saturated by a vacuum pump and a glass container (Figure 10). The samples were saturated under vacuum for 4-6 hours.



**Figure 10.** The image of water saturation apparatus

Acid etching test follows the procedures below:

- Remove the cores from the saturation container and clean up extra water on the surface. Wrap both halves of core sample with one layer of Teflon tape. Apply a thin layer of high vacuum grease on the surface to make the sample easier to be pushed into the cell.
- Glue O-rings to the slots inside the conductivity cell. Use a hydraulic jack slowly to push the cores into the conductivity cell. Keep a 0.12-in gap between the two sides of fracture, so acid can flow through the fracture .



- Assemble two pistons and keep them in place by the hydraulic jack to prevent the pistons from moving out of the cell during the acid etching test.
- Connect all the flow lines to the conductivity cell once the cell is placed at designed position. The cell is placed vertically, so the acid flows from bottom to top in order to avoid gravity effect.
- Turn on the high volume pump once all the equipment is assembled to the system. Set up the pump rate to about 0.7 liters/minute and flush the entire system.
- Use nitrogen tanks to set the cell pressure at 1000 psi and the leak-off differential pressure to 20 psi.
- Heat the system with heating jackets.
- Adjust the flowrate to 1 liter/minute, about 20 barrels/minute.
- Prepare 11 liters gelled acid in the acid mixing bucket for a 10 minutes test.
- Switch the fluid from water to acid when target temperature achieves and start to record the contact time after 1 minute.
- Record cell pressure, differential pressure along and across the fracture, leak-off volume every one minute. Deposit waste acid into a corrosion resistant barrel.
- Switched the fluid from acid to water to flush and clean the system at end of the target contact time.
- Depressure the system. Keep flushing the system until the outlet fluid shows a natural PH value of 7-7.5.

- Turn off the pump and disassemble the equipment. Remove the samples from the cell and clean up all the equipment. Figure 11 was shown the image of core samples before and after acid etching test



**Figure 11.** The image of core sample before (left) and after (right) acid etching test

### *2.2.3 Conductivity measurement procedures and calculation*

#### *Conductivity measurement procedures*

All the conductivity tests in this study are short-term conductivity measurements. Nitrogen was used to test fracture conductivities. For comparison purpose, all the core samples were tested for hydraulic fracture conductivities (unpropped and propped) before acid etching test. The procedures for unpropped, propped and acid fracture conductivity tests are similar. For unpropped fracture and acid fracture conductivity test the prepared samples do not need to be cut open to expose the fracture surface, but for propped fracture conductivity test, the sample need to be cut open in order to place proppant on fracture surfaces (**Figure 12**).



**Figure 12.** The image of prepared sample for propped conductivity test

General procedures was followed to measuring the conductivities in this study:

- Cut the windows for gas flow inlet, outlet and pressure transducers. Wrap the sample horizontally at four positions and vertically at two positions with 4 layer of Teflon tape. Apply high vacuums grease on the side of cores for easier insertion to the cell (**Figure 13**).



**Figure 13.** Prepared core sample for conductivity test

- Push the core into the conductivity cell carefully using the hydraulic jack.
- Assemble two sides piston and place the conductivity cell horizontally on the load frame. To measure acid fracture conductivity, make sure the gas flow direction follow the same direction of acid injection.
- Connect the flow lines and pressure transducers to the cell. Open the inlet valve and close the outlet valve.
- Use load frame to apply 500 psi closure pressure on the cores.
- Turn on the mass flow controller and record the flow rate baseline (usually ranges from 0.2-0.3 liters/minute).
- Close the back pressure regular and flow nitrogen into the cell until the cell pressure reaches 50 psi.
- Make sure the flow rate close to the baseline and does not exceed 0.35 liters/minute. Flow rate above 0.35 liters/minute indicates leakages within the system and the experiment must be stopped and reinstall.
- Wait 30 minutes for the entire system to reach stabilization.
- Open the backpressure regulator and adjust the flow rate, while keep the cell pressure at a fixed value (50 psi)
- Record a flow rate within 0.3-1 standard liters/minute range and its corresponding fracture differential pressure (The flow rate should not exceed 1 liter/minutes to avoid the turbulent flow and non-Darcy flow effects).
- Re-adjust the flow rate and keep the cell pressure at 50 psi. Record another set of flow rate and its corresponding fracture differential pressure. Repeat the

procedure until 4 sets of flow rates and fracture differential pressures are recorded for 500 psi closure stress.

- Increase the closure stress to next desired measure point and follow the procedure shown above to gain 4 sets of flow rates and fracture differential pressures data for this closure stress.
- Repeat the same procedures for all desired closure pressures.
- Turn off the nitrogen cylinder valve and spring valve.
- Open the backpressure regulator to release the trapped gas inside the system.
- Disassemble the conductivity cell and flow line.
- Turn off the load frame hydraulic pump and shut down the data acquisitioning system.
- Remove the core samples out of the conductivity cell using a hydraulic jack and clean the cell.

### *Conductivity calculations*

For each closure stress, the conductivity was calculated based on 4 sets of cell pressures, flow rates and fracture differential pressures.

Darcy's Law equation:

$$-\frac{dp}{dl} = \frac{\mu v}{k} \quad (2.1)$$

Since the gas mass velocity keeps constant in steady state flow and a cross sectional area, it's better to express the pressure gradient in terms of the mass velocity:

$$\frac{W}{A} = \rho v \quad (2.2)$$

Where  $W$  is mass flow rate, kg/sec;  $A$  is the cross sectional area,  $m^2$ ;  $\rho$  is gas density,  $kg/m^3$ ;  $v$  is gas velocity, m/sec.

Multiply gas density  $\rho$  on both sides of the equation (2.1) and rearrange the equation:

$$\rho \left( \frac{-dp}{dl} \right) = \rho v \frac{\mu}{k} = \frac{\mu W}{kA} \quad (2.3)$$

According to real gas law:

$$\rho = \frac{pM}{ZRT} \quad (2.4)$$

Where  $Z$  is gas compressibility factor;  $R$  is universal gas constant, J/mol-K;  $T$  is temperature, K.

Substituting equation (2.4) into equation (2.3):

$$-\frac{pM}{ZRT} dp = \frac{\mu W}{kA} dl \quad (2.5)$$

Integrating the  $dp$  and  $dl$  in equation the equation (2.5):

$$-\frac{M}{ZRT} \int_2^1 p dp = \frac{\mu W}{k A} \int_1^2 dl \quad (2.6)$$

Finally, we have:

$$\frac{M}{ZRT} \frac{(p_1^2 - p_2^2)}{2} = \frac{\mu W}{k A} L \quad (2.7)$$

The gas velocity within the fracture is equal to,

$$\frac{q}{w_f h_f} = \frac{W}{A\rho} \quad (2.8)$$

So, the final modified Darcy's law is:

$$\frac{(p_1^2 - p_2^2)M}{2ZRTL} = \frac{1}{k_f w_f} \frac{q \rho \mu}{h_f} \quad (2.9)$$

Where  $q$  is the gas flow rate, L/minute;  $p_1$  and  $p_2$  are gas flow inlet pressure and outlet pressure, respectively, psi;  $M$  is the molecular mass of gas, kg/mol;  $h_f$  is fracture width, inch;  $L$  is pressure drop length, inch; Assume temperature  $T$ , gas viscosity  $\mu$ , and gas density  $\rho$  are constants in this experiment. The parameters associate with nitrogen gas and experimental conditions in equation 2.9 are shown in **Table 1**.

**Table 1.** Fracture conductivity calculation parameters

Parameter name	Symbol	Value	Unit
Molecular mass of nitrogen	M	0.028	kg/kg mol
Fracture width	$h_f$	1.650	inch
Compressibility factor	Z	1.000	-
Universal gas constant	R	8.314	J/mol·K
Temperature	T	293.150	K
Pressure drop length	L	5.250	inch
Density of nitrogen	$\rho$	1.161	kg/m <sup>3</sup>
Viscosity of nitrogen	$\mu$	$1.759 \times 10^{-5}$	Pa·s

Variables (i.e., gas flow rate, differential pressure and absolute cell pressure) were recorded four times at each closure stress. The cell midpoint pressure measured by absolute pressure transducer is,

$$P_{cell} = \frac{P_1 + P_2}{2} \quad (2.10)$$

The differential pressure between inlet and outlet  $\Delta P$  is,

$$\Delta p = p_1 - p_2 \quad (2.11)$$

$p_1^2 - p_2^2$  is calculate as follow:

$$(p_1^2 - p_2^2) = (p_1 + p_2)(p_1 - p_2) = 2p_{cell}\Delta p \quad (2.12)$$

Therefore, at a certain closure stress, a straight line is generated by plotting  $\frac{2P_{cell}\Delta pM}{2ZRTL}$

on the y-axis and  $\frac{q\rho\mu}{h_f}$  on the x-axis. The conductivity  $k_f w_f$  at this closure was

expressed as the inverse of the straight-line slope. **Table 2** is an example calculation sheet for calculating fracture conductivity test at a certain closure stress. The calculation result was shown on **Figure 14**.

**Table 2.** An example sheet to calculate fracture conductivity

Flow Rate	P <sub>Cell</sub>	ΔP	y-axis, 2P <sub>cell</sub> ΔPM/ (2ZRTL)	x-axis, ρqμ/h <sub>f</sub>	slope from graph	k <sub>f</sub> -w
(L/min)	(psi)	(psi)	(1/m <sup>3</sup> )	-	-	(md-ft)
0.075	50	1.74	4.44E+05	6.09E-10		
0.095	50	2.31	5.92E+05	7.72E-10	8E+14	4.16
0.118	50	3.01	7.75E+05	9.58E-10		
0.129	50	3.37	8.69E+05	1.05E-09		



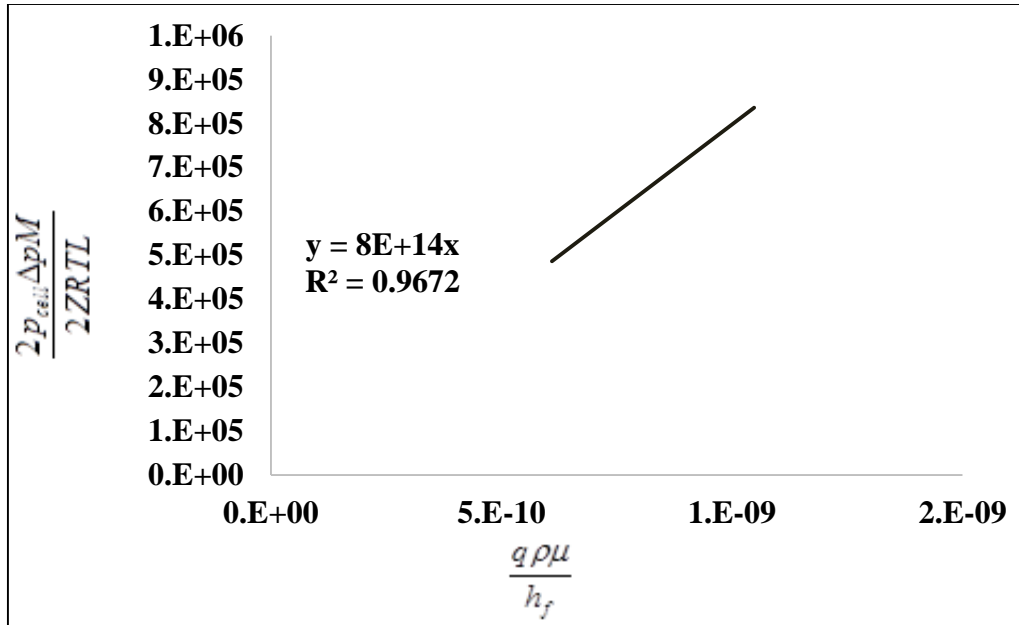


**Figure 14.** An example plot to calculate fracture conductivity

#### 2.2.4 Fracture surface characterization

Fracture surface characterizations were done on the core samples before and after acid etching test to provide total etching volumes, ideal fracture widths after acid etching test, and acid etching patterns, for better evaluation of acid etching performance.

Before acid etching test, surface topography were taken for both halves of the sample. First, the sample was placed on the movable table with fracture facing up. Computer software controlled the table to move back and force. Laser sensor recorded the sample surface topography, which is the vertical height (z direction) at different horizontal positions (x and y direction).

After acid etching test, surface topography were taken once again for both halves of the sample. Subsequently, the surface changes on both sides of the fracture surface

before and after acid treatment were calculated by Matlab. The total acid etching volume was given by adding up the etching volumes on both sides of the sample. Additionally, the computer program provided 3-D images of the sample surface changes to illustrate the acid etching patterns. **Figure 15** is an example of surface profile changes before and after acid etching for both sides of fracture. The surface profiles clearly show acid etching pattern.

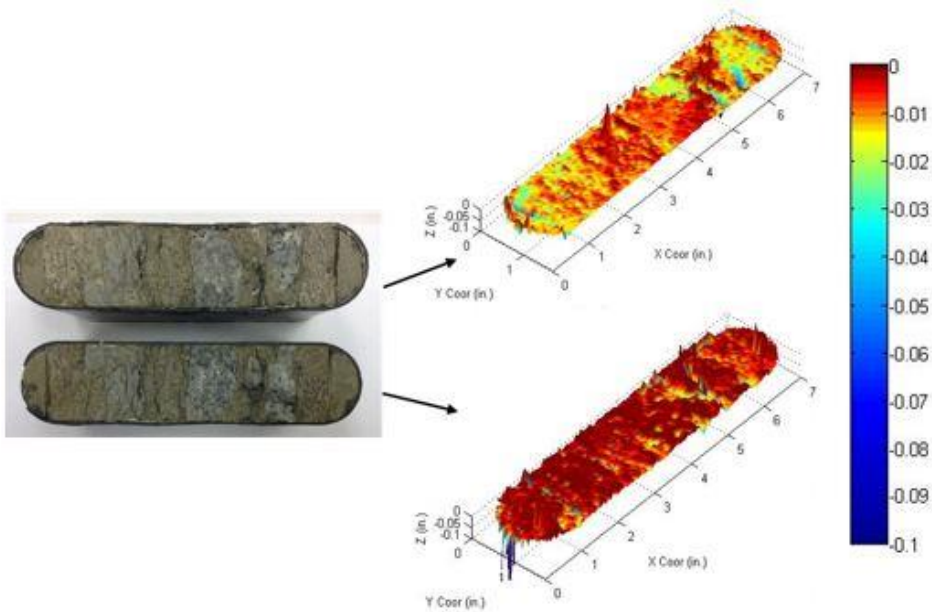


**Figure 15.** An example of surface profile generated by Matlab

## CHAPTER III

### EXPERIMENTAL RESULTS AND DISCUSSION

#### **3.1 Field sample description**

Tarim oilfield is located in Tarim basin of northeast China. The basin is the largest inland basin in China, which is about 870 miles long from east to west and about 323 miles wide from north to south (**Figure 16**) (Kmusser, 2008).

The stimulation technologies were widely used in Tarim carbonate reservoirs, including matrix acidizing, acid fracturing, and hydraulic fracturing with proppant. The main challenges of stimulating the wells in the field are: 1) Heterogeneous and ultra-deep formation; 2) high temperature and pressure environment.

For studying purpose, three types of formation were classified in this field, including connected caves, vuggs with natural fractures, and tight matrix with fissures. This research was targeted at dispersed vuggy formation with natural fractures and all the studied core samples were taken from this formation. The main objective of this study is to test the feasibility of acid fracture stimulation on this type of formation and to provide suggestions of the optimum fracturing design and treatment conditions.



**Figure 16.** Tarim basin location map (Knusser, 2008)

Five core samples from three horizontal wells from the dispersed vuggy formation were tested in this study. The well information were shown in **Table 3**.

**Table 3.** Formation characteristics of investigated well

Well	MD ft	TVD ft	Temperature °F	Pressure psi
1	23,343	19,872	286	10,341
2	23,346	17,818	275	9,862
3	21,998	16,213	262	8,673

Core sample A is from well 1, core sample B and C are from well 2, and core sample D and E are from well 3. **Table 4** shows the rock properties of the tested sample.

**Table 4.** Rock properties of the tested samples

Well	Sample	Lithology	Perm md	Porosity %	Young's Modulus GPa
1	A	75% dolomite and 25% calcite	0.006	2.7	57.5
2	B	100% calcite	0.002	1.8	44.34
	C	100% calcite	0.002	1.8	44.34
3	D	95% Calcite, 1% dolomite and 4% quartz	0.004	2.9	44.34
	E	100% Calcite	0.006	2.6	46.53

### 3.2 Acid etching test results

#### 3.2.1 Well 1 sample acid etching test results

Acid etching test was conducted on core sample A. The cell was pressurized to 1000 psi during the test for all the acid etching tests to ensure the produced CO<sub>2</sub> stay dissolving in the solution. In order to achieve a leak-off pressure of 20 psi, the backpressure was set to 980 psi. The flow line and cell were heated by the heating jackets to 130 °F. 20% gelled acid was injected. The acid contact time is 10 minutes with an injection rate of 1 liter/minute. During the acid injection, pressures, temperatures at the upstream and downstream, and the leak-off volume were recorded.

To compare the fracture face topography of each sample, two sides of the sample were scanned with a profilometer before and after the acid etching experiment. The images of the sample surface after acid etching along with the difference in surface profile before and after acid injection are shown in **Figure 17**. The color scale corresponds to the depth of asperity with values ranging from 0 to 0.1 inches.

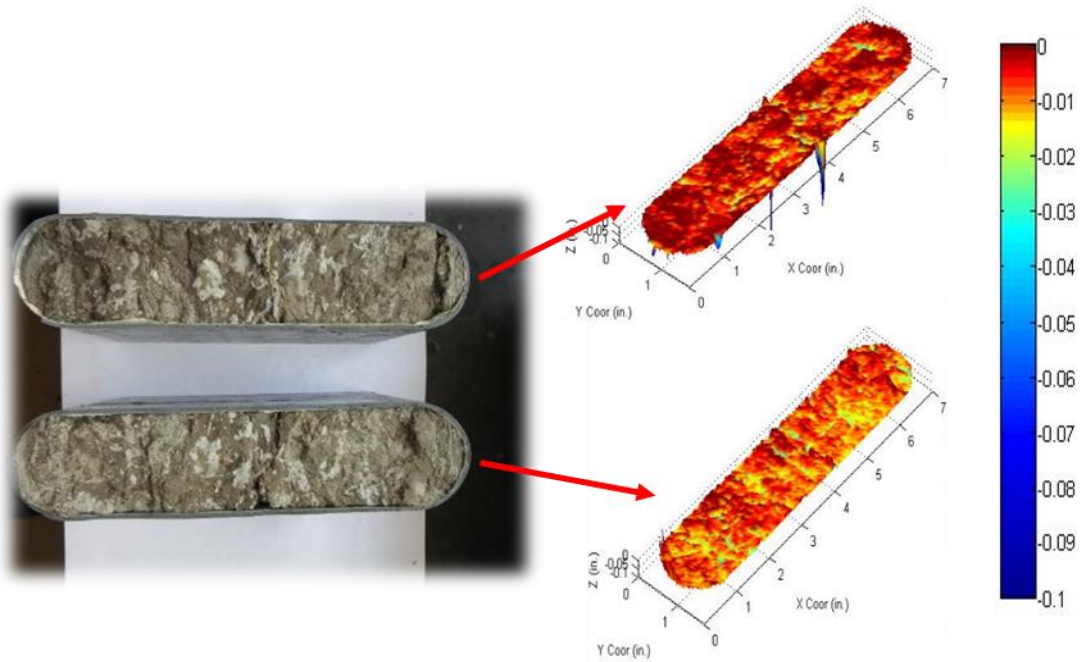


**Figure 17.** The images of sample A surface profile changes before and after acid etching

The volumes of the dissolved rock of sample A is  $0.145 \text{ in}^3$ , it is less than the rest of tested samples. The poor acid reaction was caused by the high percentage of the dolomite composition (see **Table 3**). The photo of the fracture surface after acid etching clearly showed the areas that were removed by acid. The difference of fracture surface profiles before and after the acid etching test is small on both fracture surfaces. Moreover, the surface etching patterns are uniform and no identical acid-etched channel was created (**Figure 17**). The total leak-off volume was 176 ml. It's comparably high than a typical acid etching test were done in the same lab using the same gelled acid system (it usually within 10-100ml range) (reference on Melendez et al, Pournik et al, Almomen et al). Most of the leak-off acid was caused by the crack in the middle of the fracture.

### 3.2.2 Well 2 samples acid etching test results

The experimental results of sample B and sample C are presented in this section.

For sample B, the flow line and cell were heated up by the heating jackets to 150 °F. Other experimental conditions for acid injection were kept the same with the test were done on sample A. The images of the sample surface after acid etching along with the difference in surface profile created by acid etching are shown in **Figure 18**. The same color scale mentioned in section 3.2.1 is used for the profiles of both sample B and C.

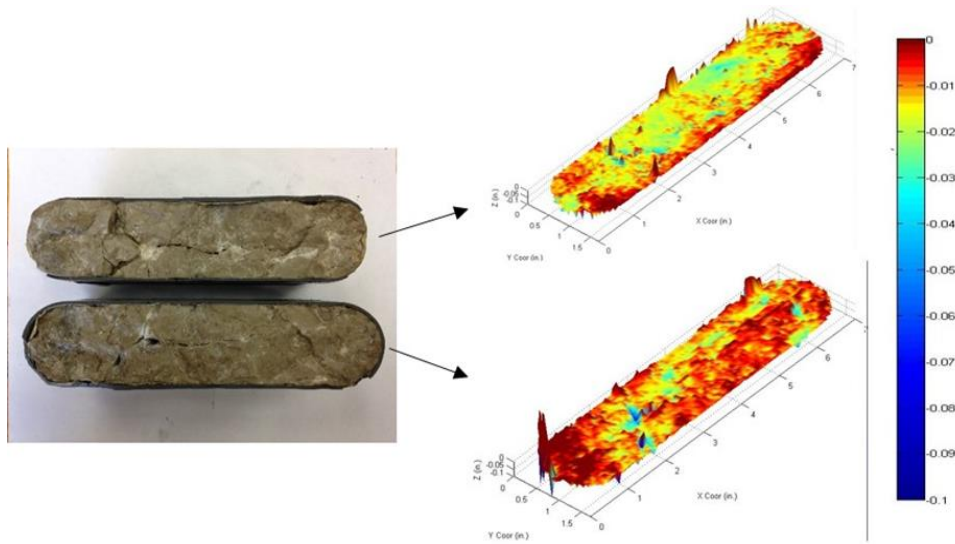


**Figure 18.** The images of sample B surface profile changes before and after acid etching

The dissolved rock volumes of the sample B is  $0.241 \text{ in}^3$ , and it is a typical value observed in limestone acid etching test (10-100 ml). Most parts of the surface reacted with acid (see the photo in **Figure 18**). The surface profile differences between before

and after acid etching test are apparent. Moreover, one clear acid etching channel can be observed on the both sides of the fracture (see the surface profile in **Figure 18**). The total leak-off volume was 535ml, it was higher than typical tests. The high leak-off was also caused by the nature fractures in the sample.

For sample C, the flow line and cell were heated up by heating jackets to 125 °F. The acid concentration, injection rate, and contact time were also kept the same with the test were done on sample A. The images of the sample surface after acid etching along with the difference in surface profile created by acid etching are shown in **Figure 19**.

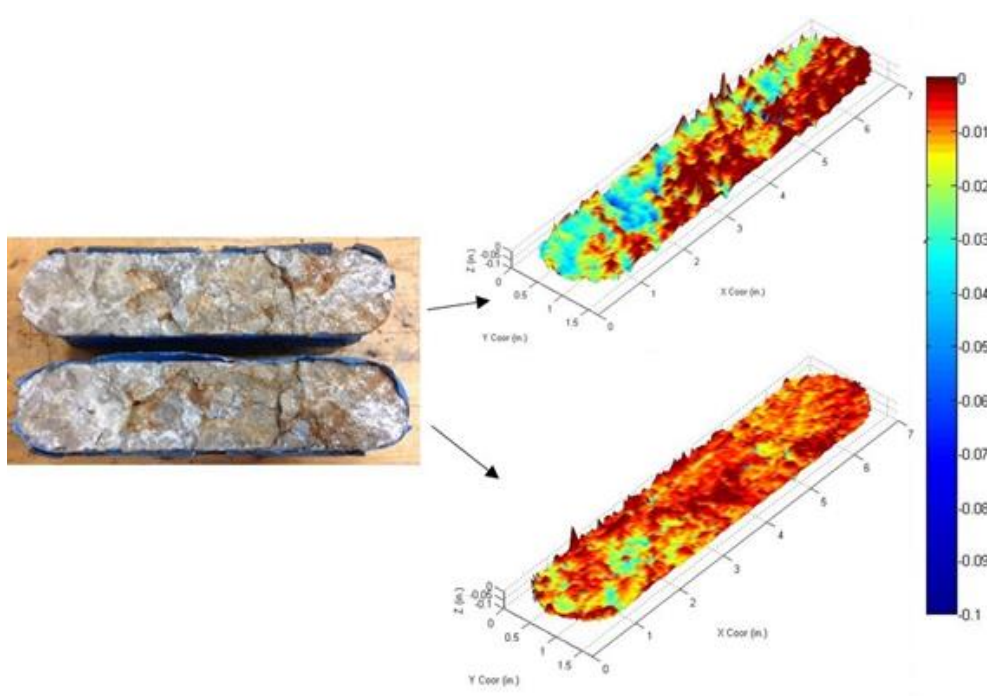


**Figure 19.** The images of sample C surface profile changes before and after acid etching



The volumes of the dissolved rock of sample C is  $0.224 \text{ in}^3$ , it is similar with the dissolved volume of sample B. Most parts of the surface reacted with acid (see the photo in **Figure 19**). The surface profile differences between before and after acid etching test are apparent, and one deep acid etching channel can be observed on the top side surface (see the surface profile in **Figure 18**). The total leak-off volume was 39ml, it was a typical value for 10 minutes limestone etching test.

### 3.2.3 Well 3 sample acid etching test results

Acid injection were conducted on core sample D and E under same condition, with temperatures of  $125 \text{ }^\circ\text{F}$ , injection rate of  $1 \text{ L/min}$  and contact time of 10 minutes.

The images of the sample D surface differences before and after acid injection are shown in **Figure 20**.

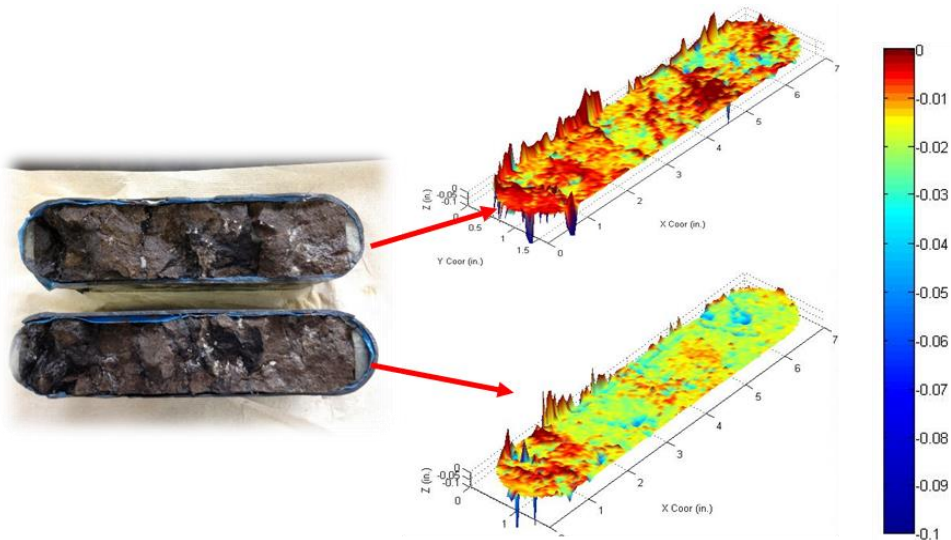


**Figure 20.** The images of sample D surface profile changes before and after acid etching

The volumes of the dissolved rock of sample D is 0.414 in<sup>3</sup>. The acid-etched volume was the highest among all the tested samples, it was caused by the rough fracture surface (see the photo in **Figure 20**). The surface profile differences between before and after acid etching test are apparent. Acid removed most convex parts of the surface, but the concave parts of the surface was not etched significantly. No etched channel was found on both sides of fracture (see the surface profile in **Figure 20**). The total leak-off volume was 153 ml, it is slightly higher than typical laboratory tests on limestone sample (10-100ml). Sample D was broke into pieces during the rock preparation procedure, due to the complex mineralogical compositions (see **Table 3**). Although the sample was glued back in shape by using epoxy, minor fractures and small holes still existed in the rock. Acid leaked off through these fractures and holes.

Sample E had the roughest surface face and it exceed the measurement range of the profilometer, the surface profile for E failed to be conducted. The total leak-off volume was 245 ml. The experimental conditions for the acid etching experiments are summarized in **Table 5**.

**Table 5.** The volumes of the dissolved rock

<b>Well/Sample</b>	<b>Temperature (°F)</b>	<b>Contact time (mins)</b>	<b>Dissolved volume (in<sup>3</sup>)</b>
1(A)	130	10	0.145
2(B)	150	10	0.241
2(C)	125	10	0.224
3(D)	125	10	0.414
3(E)	125	10	-

### **3.3 Fracture conductivity test results**

#### *3.3.1 Well 1 sample fracture conductivity test results*

Three conductivity tests were done on core sample A from well 1, unpropped hydraulic fracture conductivity test, propped hydraulic fracture conductivity test and acid fracture conductivity test.

Unpropped hydraulic fracture conductivity test was done following the procedures in section 2.2.3. The conductivities were measured under closure stress of 500, 1000 and 2000 psi. At 2000 psi stress, the measured conductivity was about 11 md-ft.

For the propped hydraulic fracture conductivity test, 30/50 mesh-size ceramic proppant at concentration of 0.2 lb/ft<sup>2</sup> was manually placed and evenly distributed on the fracture face of the sample. Then, the propped conductivity measurement followed the same procedures of unpropped fracture test. The round-shape ceramic proppant was rolling from the angular high parts of the surface (hills) and was accumulating in the low part of the surface (valleys). From the visual inspection of the sample's fracture faces, the valleys accumulated 5-7 layers of proppant, while the hills had only 0-3 layers. Proppant crushing was observed after the conductivity test, it occurred mainly along the surface slopes. The angular surface asperities crushed the ceramics. The sound of the cracking proppant was heard during the experiment when increasing stress from 1000 psi to 3000 psi.

The acid fracture conductivity measurement was done for closure stress of 1000, 1500, 2000, 3000, 4000, 5000, 6000 and 7000 psi. The fracture conductivity was

calculated by using Modified Darcy's law based on four data points recorded at each closure stress, and the measurements were repeated for different closure stresses. **Table 6** showed the experimental condition of conductivity tests on sample A. The fracture conductivity data at different closure stress for acid fracture experiment along with unpropped and propped experiments are presented on **Figure 21**.

**Table 6.** The experimental condition of conductivity tests on sample A

<b>Test name</b>	<b>Proppant type</b>	<b>Proppant Concentration lb/ft<sup>2</sup></b>	<b>Temperature °F</b>	<b>Closure Stress psi</b>
Unpropped	None	0	68	500, 1000, 2000 3000 and 4000
Propped	30/50 mesh ceramic	0.1	68	1000, 2000, 3000, 4000, 5000 and 7000
Acid	None	0	68	500, 1000, 2000, 3000, 4000, 5000 and 7000

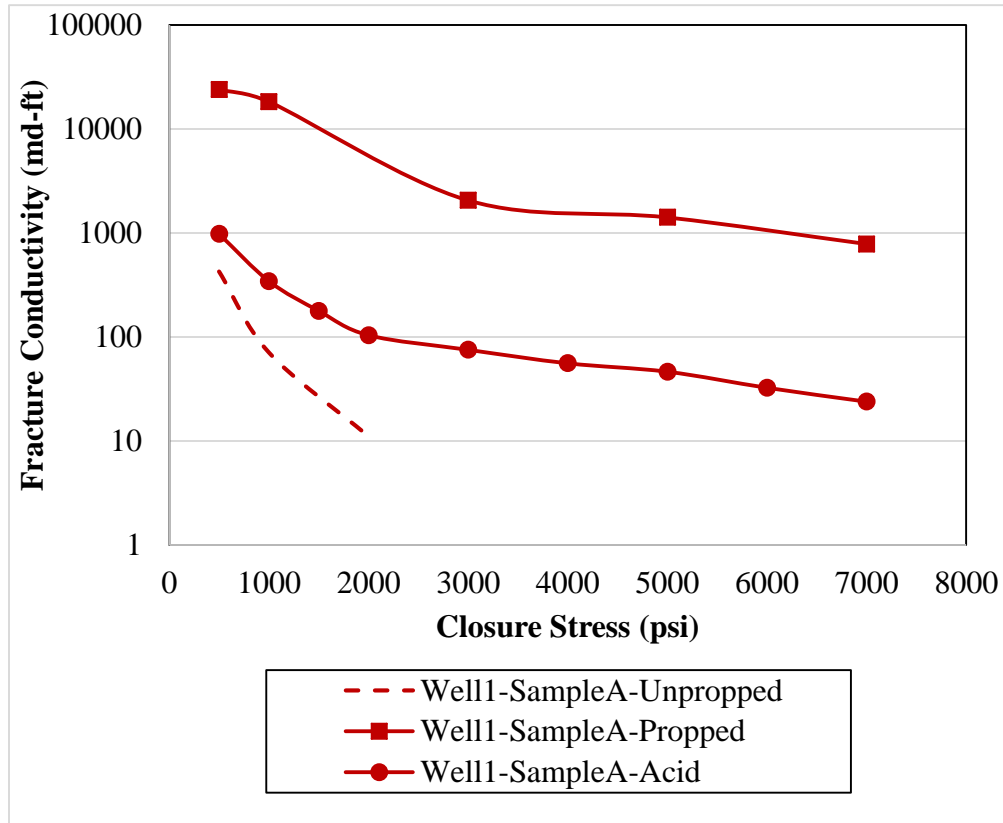


**Figure 21.** Sample A fracture conductivity data at different closure stress for acid fracture experiment along with unpropped and propped experiments

The propped fracture acid fracture conductivities are higher than unpropped fracture conductivities at all closure stresses, so both well stimulation techniques can improve the well performance. Furthermore, the propped fracture conductivities are one order of magnitude higher than acid fracture conductivities. The young's modulus is high due to the large percentage of the dolomite composition. The fracture surface can even crush the ceramic proppant. Therefore, the propped fracture conductivity can retain 800 md-ft at 7000 psi closure stress. Although acid did not remove large amount of rock during the dynamic etching test (see **Table 5**), the hard rough surface still help the

conductivity to retain in high closure stress. From 3000 psi to 7000 psi, the conductivity only dropped about 50 md-ft. At 7000 psi closure stress, the conductivity was about 23 md-ft.

### *3.3.2 Well 2 sample fracture conductivity test results*

Two core samples from the well 2 (sample B and C) were selected for this experimental study. Three conductivity tests were done on each sample, unpropped hydraulic fracture conductivity test, propped hydraulic fracture conductivity test and acid fracture conductivity test.

The unpropped fracture conductivity was measured under closure stress of 500, 1000, 2000, 3000, and 4000 psi for both sample B and C. The test on sample B obtained a conductivity of 42 md-ft at 500 psi stress and 1 md-ft at 7000 psi. For sample C, the conductivity were one order of magnitude higher than sample B. It was 534 md-ft at 500 psi stress and 11 md-ft at 7000 psi.

For propped fracture conductivity measurement on both sample B and C, 30/50 mesh-size ceramic proppant were manually placed and evenly distributed on the fracture face of the samples. The experimental procedures were similar to the unpropped fracture conductivity measurements. Two different proppant concentrations were tested for the Sample B. First, 0.2 lb/ft<sup>2</sup> concentration of proppant was used to measure fracture conductivity. However, during the test, the pressure drop across the propped fracture was unreliably small at the maximum flow rate (9 L/min) at closure stress of 4000 psi. It may be caused by the system leakage. Therefore, the proppant concentration was decreased to 0.1 lb/ft<sup>2</sup> for the second test on sample B, and the conductivity experiment was

measured under closure stress of 2000, 3000, 4000, 5000, and 7000 psi. The fracture conductivity was calculated from the four data points recorded at each closure stress. For sample C, 0.1 lb/ft<sup>2</sup> proppant concentration was used for the conductivity test. The propped fracture conductivity of core sample C was higher than that of sample B at all closure stresses.

The acid fracture conductivity measurements followed the same procedures of unpropped hydraulic fracture tests. The experiment was done on sample B under closure stress of 500, 1000, 2000, 3000, 4000, 5000, 6000 and 7000 psi. Similarly, the experiment was done on sample C under closure stress of 500, 1000, 2000, 3000, 4000, 5000 and 7000 psi. The measurements were repeated for different closure stresses. **Table 7** showed the experiment condition of conductivity tests on sample B. **Table 8** showed the experiment condition of conductivity tests on sample C. The fracture conductivity data at different closure stress for acid fracture experiment along with unpropped and propped experiments are presented in **Figure 22**.

**Table 7.** The experimental condition of conductivity tests on sample B

<b>Test name</b>	<b>Proppant type</b>	<b>Proppant Concentration lb/ft<sup>2</sup></b>	<b>Temperature °F</b>	<b>Closure Stress psi</b>
Unpropped	None	0	68	500, 1000, 2000 3000 and 4000
Propped	30/50 mesh ceramic	0.1	68	2000, 3000, 4000, 5000, and 7000
Acid	None	0	68	500, 1000, 2000, 3000, 4000, 5000 6000, and 7000

**Table 8.** The experimental condition of conductivity tests on sample C

<b>Test name</b>	<b>Proppant type</b>	<b>Proppant Concentration lb/ft<sup>2</sup></b>	<b>Temperature °F</b>	<b>Closure Stress psi</b>
Unpropped	None	0	68	500, 1000, 2000 3000 and 4000
Propped	30/50 mesh ceramic	0.1	68	1000, 2000, 3000, 4000, 5000, and 7000
Acid	None	0	68	500, 1000, 2000, 3000, 4000, 5000, and 7000



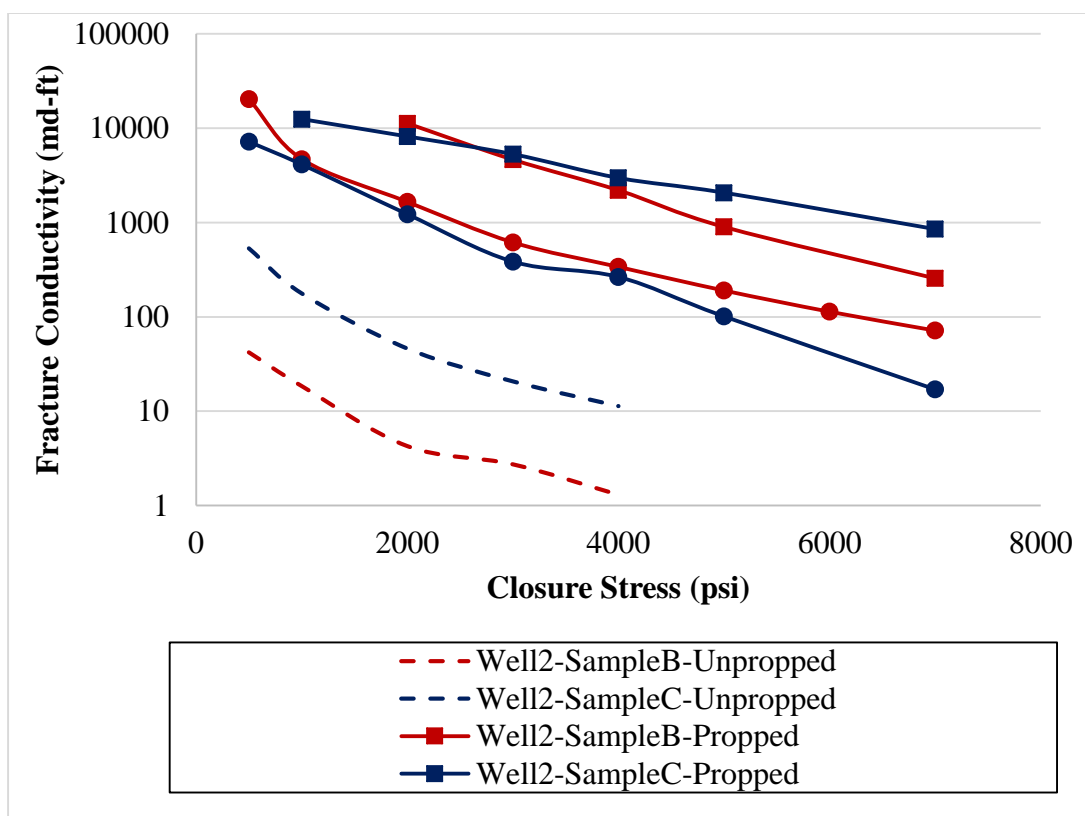


**Figure 22.** Sample B and C fracture conductivity data at different closure stress for acid fracture experiment along with unpropped and propped experiments

For both samples from well 2, the propped and acid fracture conductivities are both higher than unpropped fracture conductivities at all closure stresses, so both well stimulation techniques can improve the performance for this well. The propped fracture conductivities at 7000 psi of for sample B and sample C are 255 md-ft and 852 md-ft, respectively. The unpropped fracture conductivities for sample C are much higher than sample B at all closure stresses. In addition, the propped fracture conductivity curve for sample B at all closure stresses. In addition, the propped fracture conductivity curve for sample C is not as steep as sample B. Therefore, the system might have leakage during the tests on sample C. The acid fracture conductivity values for sample B and C are close

till closure stress reach 4000 psi. After 4000 psi, the conductivity of sample C declines fast than the conductivity of sample B does, but they still stay in the same order of magnitude. At 7000 psi, the rained conductivities for sample B fracture and sample C fracture are 71 md-ft and 17 md-ft, respectively.

### *3.3.3 Well 3 samples fracture conductivity test results*

Two core samples from the well 3 (sample D and E) were tested for conductivities following the same experimental procedure that were used on sample A, B and C.

The unpropped hydraulic fracture conductivity test were done under closure stress of 500, 1000, 2000, 3000 and 4000 psi for sample D and under closure stress of 500 and 1000 psi for sample E.

Closure stress of 500, 1000, 2000, 3000, 5000 and 7000 psi were chosen to test propped fracture conductivity on both sample D and E. The rough fracture surface propped by 20/40 mesh sand at concentration of 0.2 lb/ft<sup>2</sup> provided high conductivity for both sample D and E.

For acid fracture conductivity measurement, the experiment was conducted for closure stress of 500, 1000, 2000, 3000, 5000 and 7000 psi. The fracture conductivity was estimated with the four data points recorded at each closure stress.

**Table 9** showed the experiment condition of conductivity tests on sample D. **Table 10** showed the experiment condition of conductivity tests on sample E. The fracture conductivity data at different closure stress for acid fracture experiment along with unpropped and propped experiments are presented in **Figure 23**.

**Table 9.** The experimental condition of conductivity tests on sample D

<b>Test name</b>	<b>Proppant type</b>	<b>Proppant Concentration lb/ft<sup>2</sup></b>	<b>Temperature °F</b>	<b>Closure Stress psi</b>
Unpropped	None	0	68	500, 1000, 2000 3000 and, 4000
Propped	20/40 mesh sand	0.2	68	500, 1000, 2000, 3000, 5000, and 7000
Acid	None	0	68	500, 1000, 2000, 3000, 5000, and 7000

**Table 10.** The experimental condition of conductivity tests on sample E

<b>Test name</b>	<b>Proppant type</b>	<b>Proppant Concentration lb/ft<sup>2</sup></b>	<b>Temperature °F</b>	<b>Closure Stress psi</b>
Unpropped	None	0	68	500 and 1000
Propped	20/40 mesh sand	0.1	68	500, 1000, 2000, 4000, 6000, and 7000
Acid	None	0	68	500, 1000, 2000, 3000, 5000, and 7000

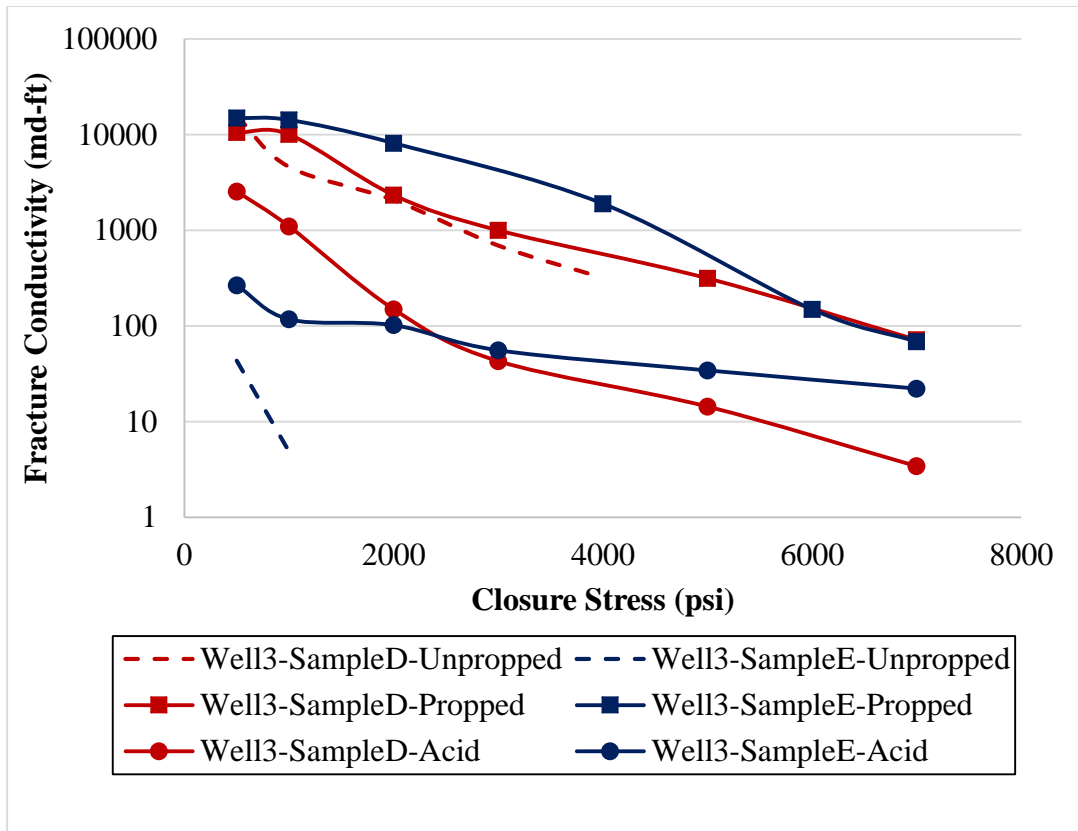


**Figure 23.** Sample D and E fracture conductivity data at different closure stress for acid fracture experiment along with unpropped and propped experiments

Unpropped fracture conductivity test on sample D gave abnormally high values. Therefore, the experiment on sample E was conducted to verify the unpropped fracture conductivity. At 1000 psi closure stress, the conductivity of sample E was about 5 md-ft. The propped fracture conductivities of sample D and E gives close values at 7000 psi closure stress, the conductivities were 72 md-ft and 69md-ft, respectively. However, acid fracture conductivity test on sample D and E shows different results. Sample D fracture conductivity declines faster than the Sample E does. At 7000 psi closure stress, the conductivities of sample D was 3 md-ft, whereas the conductivity of sample E was 22

md-ft. Sample D had the most acid-etched volume compare with all other tested samples in this research (see **Table 5**). The over-etched fracture surfaces maybe the reason that caused sample D fracture conductivity declined faster and closed earlier, since over etching can lower the fracture surface rock strength. Additionally, the rough fracture surface might affect the fracture conductivity by resisting the fluid flow through the fracture (**Figure 24**).

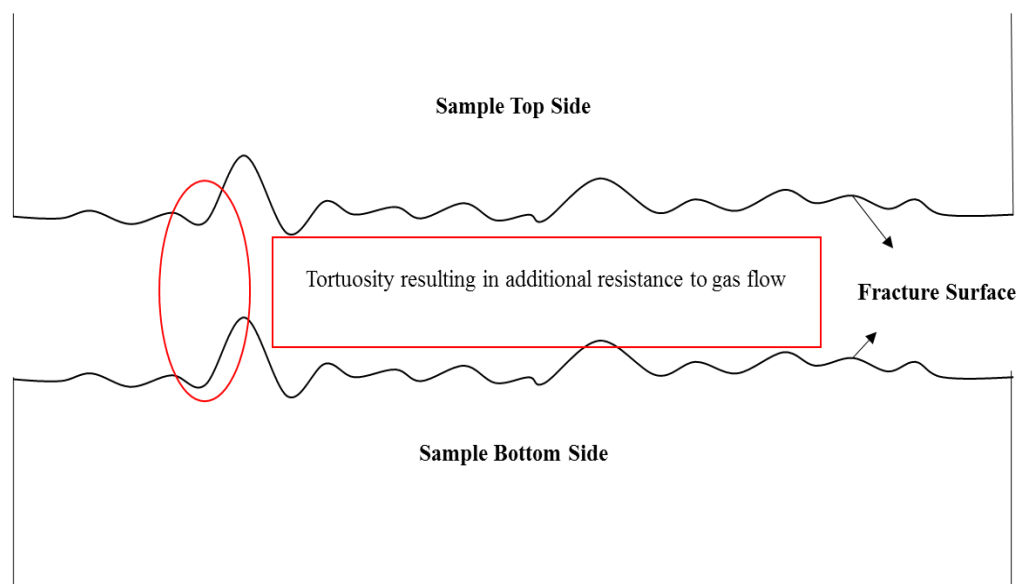


**Figure 24.** The effect of rough surface on fluid flow

### 3.3.4 Conductivity measurement comparisons of three wells

The experimental results shown that heterogeneity and mineralogical composition have great impact on propped fracture conductivities (**Figure 25**).

Sample from well 1 contains mainly dolomite and has the highest young's modulus (see **Table 4**), so proppant was able to create a fracture conductivity of 800 md-ft under 7000 psi closure stress.

Samples (B and C) from well 2 are pure limestone, they have lower young's modulus than sample A does. Since system leakage was identified during sample C propped fracture conductivity test, so sample B test result was used to represent well 2 propped fracture conductivity behavior. Proppants on sample B fracture surface was able to create to create a fracture conductivity of 255 md-ft under 7000 psi closure stress.

Samples from well 3 have the most complex mineralogical composition, highest heterogeneity, and most rough fracture surface compared with samples from well 1 and 2. Although bigger size proppant was used to test well 3 samples (proppant size 30/50 was used for well 1 and 2 samples, proppant size 20/40 was used for well 3 samples), the tested two samples have the least propped fracture conductivities at 7000 psi closure stress compare to the samples from well 1 and 2. According to the observation, the proppant was mostly accumulating in the low part of the rough surface (valleys) after the conductivity test.

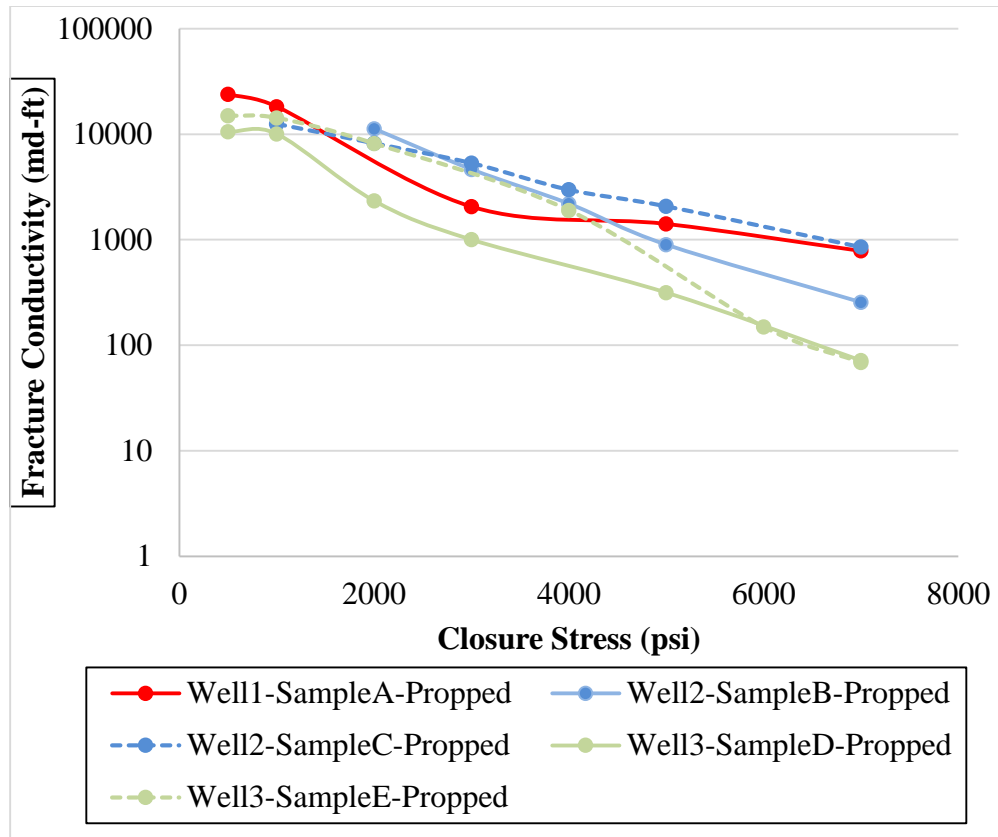


**Figure 25.** Sample A-E fracture conductivity data at different closure stress for propped fracturing experiments

The acid fracturing experiments were done under similar conditions for five samples and the conductivity curves was generated in **Figure 26**.

Sample A from well 1 has the most flat acid fracture conductivity curve among all the tested samples. It indicates that, with the closure pressure increasing, the fracture conductivity of sample A does not change as much as other sample does. The reason is as follows: 1) sample A has the least acid-etching volume, so the initial conductivity of sample A at 500 psi is low; 2) sample A rock has the highest young's modulus, so the fracture surface can better keep the acid created conductivity than other sample rocks.

Acid fracture conductivities of well 2 samples (B and C) are higher than other samples till closure stress reaches 6000 psi, it is the result of the channeling patterns of sample B and C fracture surfaces (discussed in section 3.2.2). However, sample B and sample C rocks cannot keep their conductivities as good as sample A rock does at high closure stress. Therefore, conductivity curves of sample B and C decline faster than sample A curve.

The conductivity of sample D from well 3 starts to drop rapidly after the closure stress reaches 3000 psi, and it has the lowest conductivity among all five samples at 7000 psi. It might be caused by over-etched fracture surface and the roughness of the fracture that was discussed in section 3.3.3 (see **Figure 24**). Sample E is also from well 3, but it has different mineralogical composition comparing with sample D. Sample E is pure calcite and has higher young's modulus than sample D. Therefore, conductivity curves for these two samples are different.



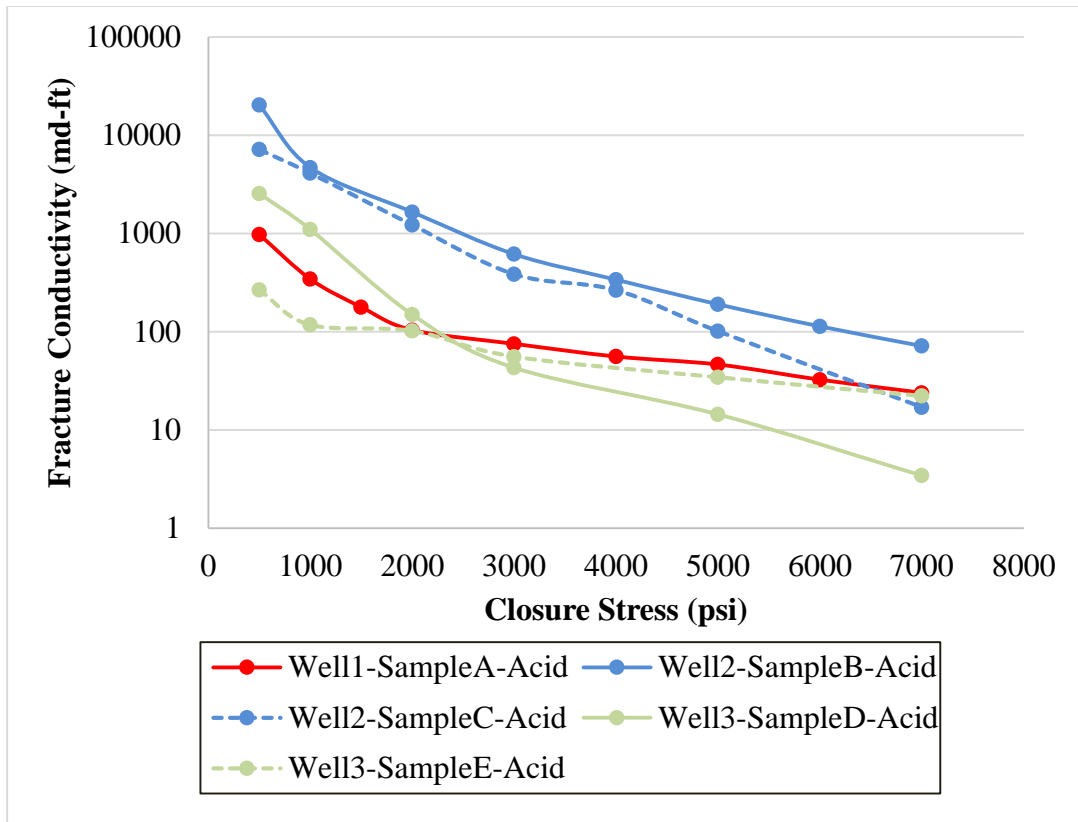


**Figure 26.** Sample A-E fracture conductivity data at different closure stress for propped fracturing experiments

### 3.4 Productivity calculation results

According to well 1 conductivity test results, propped fracturing treatment gives  $k_{fw}=782$  md-ft under effective closure stress of 7000 psi. Assume the reservoir permeability  $k=0.02$  md, fracture half-length is  $x_f= 350$  ft. the fracture dimensionless conductivity,  $C_{fD}$ , can be calculated according to Cinco-Ley and Samaniego (1981) equation,

$$C_{fD} = \frac{k_f w}{k x_f} = \frac{782}{(0.02)(350)} = 112 \quad (3.1)$$

Therefore, from the equation developed by Meyer and Jacot (2005),

$$r_w' = \frac{x_f}{\frac{\pi}{C_{fD}} + 2} = \frac{350}{\frac{\pi}{112} + 2} = 173 \text{ ft} \quad (3.2)$$

Since, the wellbore radius is 0.28 ft, the equivalent skin effect,  $s_f$ ,

$$s_f = -\ln \frac{r_w'}{r_w} = -\ln \frac{173}{0.28} = -6.42 \quad (3.3)$$

Assume the reservoir radius is 900 ft and formation thickness is 150 ft. The post-fracture productivity index can be estimated for propped fracturing treatment. Calculate the dimensionless productivity index by using single-phase pseudosteady-state equation,

$$J_{D_{pss}} = \frac{1}{\ln \frac{r_e}{r_w} - 0.75 + s_f} = \frac{1}{\ln \frac{900}{0.28} - 0.75 - 6.42} = 1.109 \quad (3.4)$$

For horizontal well with transverse fracture, choke effect needs to be considered, denoted as “choke skin” (Mukherjee and Economides, 1991),

$$s_c = \frac{kh}{k_f w} \left[ \ln \left( \frac{h}{2r_w} \right) - \frac{\pi}{2} \right] = \frac{(0.02)(150)}{782} \left[ \ln \left( \frac{150}{(2)(0.28)} \right) - \frac{\pi}{2} \right] = 0.015 \quad (3.5)$$

The dimensionless productivity index of the transverse fracture intersect with a horizontal well ( $J_{DTH}$ ) can be obtained by (Wei and Economides, 2005),

$$J_{DTH} = \frac{1}{\frac{1}{J_{D_{pss}}} + s_c} = \frac{1}{\frac{1}{1.109} + 0.015} = 1.091 \quad (3.6)$$

Similarly, assume acid fracture has the same fracture half-length with propped fracture. Then, the post-fracture productivity index for acid fracturing treatment can be calculated,

$$C_{fD} = \frac{k_f w}{k x_f} = \frac{24}{(0.02)(350)} = 3 \quad (3.7)$$

$$r_w' = \frac{x_f}{\frac{\pi}{C_{fD}} + 2} = \frac{350}{\frac{\pi}{3} + 2} = 120 \text{ ft} \quad (3.8)$$

$$s_f = -\ln \frac{r_w'}{r_w} = -\ln \frac{120}{0.28} = -6.06 \quad (3.9)$$

$$J_{Dpss} = \frac{1}{\ln \frac{r_e}{r_w} - 0.75 + s_f} = \frac{1}{\ln \frac{900}{0.28} - 0.75 - 6.06} = 0.791 \quad (3.10)$$

$$s_c = \frac{kh}{k_f w} \left[ \ln \left( \frac{h}{2r_w} \right) - \frac{\pi}{2} \right] = \frac{(0.02)(150)}{24} \left[ \ln \left( \frac{150}{(2)(0.28)} \right) - \frac{\pi}{2} \right] = 0.502 \quad (3.11)$$

$$J_{DTH} = \frac{1}{\frac{1}{J_{Dpss}} + s_c} = \frac{1}{\frac{1}{0.791} + 0.502} = 0.566 \quad (3.12)$$

The productivity ratio is,

$$\frac{J_{DTH} PF}{J_{DTH} AF} = \frac{1.091}{0.566} = 1.9 \quad (3.9)$$

Use the same method to calculate productivity index for well 2 and well 3, the results were shown in **Table 11**.

**Table 11.** Calculated post-fracture productivity index

<b>Well</b>	<b>J<sub>Dpss</sub> (Prpped)</b>	<b>J<sub>Dpss</sub> (Acid)</b>	<b>S<sub>c</sub> (Propped)</b>	<b>S<sub>c</sub> (Acid)</b>	<b>J<sub>DTH</sub> (Propped)</b>	<b>J<sub>DTH</sub> (Acid)</b>	<b>J_P/J_A</b>
1	1.109	0.791	0.015	0.502	1.091	0.566	1.927
2	1.111	0.721	0.014	0.709	1.093	0.477	2.292
3	1.085	0.682	0.038	0.861	1.041	0.429	2.425

From above calculation, a single propped fracture has about 2 times higher post-fracture productivity index than a single acid fracture for 3 tested wells. The productivity index ratio between propped fracture and acid fracture ranges from 1.9 to 2.4. Therefore, higher production rate and ultimate recovery can be expected from proppant-fracture treatment than acid fracture treatment.

## CHAPTER IV

### CONCLUSIONS AND RECOMMENDATIONS

#### 4.1 Conclusions

Five rock samples, Sample A, B, C, D, and E were tested for conductivity under specified conditions downscaled from the field treatment conditions. The following conclusion for this study were given based on the experimental results:

1. The conductivity test results show that propped fracturing is a better method than acid fracturing for stimulating well 1, 2 and 3. In deep formation, acid fracturing cannot create enough conductivity under high closure stress.
2. Mineralogical composition appears to have significant impact on propped hydraulic fracture conductivity. Samples with higher dolomite percentage can obtain higher fracture conductivity from the proppant under the same closure stress in this study.
3. Fracture surface channels that created by acid can help to improve the fracture conductivity under low closure stresses. With the increasing of closure stress, the strength of surface rock starts to dominate the fracture conductivity.
4. The heterogeneity of the formation rock has a direct impact on the fracture surface roughness. In this research, the sample has more complex mineralogical compositions, the fracture has rougher surfaces. The rough fracture surfaces can influence the conductivity test results.

## **4.2 Recommendations**

To better understand the conductivity test result, rock mechanical properties should be measured in the lab using the same rock sample.

Choosing better stimulate strategies and optimizing experimental conditions. For example, higher acid concentration and longer contact time was recommended to test on samples from well 1, since the rock has high dolomite composition (up to 75%).

## REFERENCES

- Abass, H.H., Al-Mulhem, A.A., and Mirajuddin, K.R. Acid Fracturing or Proppant Fracturing in Carbonate Formation? A Rock Mechanic's View. Paper SPE 102590 presented at the 2006 SPE Annual Technical Conference and Exhibition, San Antonio, Texas, 24-27 September.
- Almomen, A.M. The Effects of Initial Condition of Fracture Surfaces, Acid Spending, and Type on Conductivity of Acid Fracture. M.S. Thesis, Texas A&M University, College Station, Texas (2013).
- Anderson, M.S. and Fredrickson, S.E. 1989. Dynamic Etching Tests Aid Fracture-Acidizing Treatment Design. *SPE Prod Eng* 4 (4): 443-449. SPE-16452-PA. <http://dx.doi.org/10.2118/16452-PA>.
- Beg, M.S., Kunak, A.O., Gong, M. et al. 1998. A Systematic Experimental Study of Acid Fracture Conductivity. *SPE Prod & Fac* 13 (4): 267-271. SPE-52402-PA. <http://dx.doi.org/10.2118/52402-PA>.
- Cinco-Ley, H., and Samaniego, F. Transient Pressure Analysis for Fracture Wells. *JPT* 1749-1766 (September 1981).
- Deng, J., Mou, J., Hill, A.D., and Zhu, D. 2012. A New Correlation of Acid-Fracture Conductivity Subject to Closure Stress. *SPE Prod. & Oper.* 27(2): 158-169.
- Gong, M., Lacote, S., and Hill, A.D. New Model of Acid-Fracture Conductivity Based on Deformation of Surface Asperities. Paper SPE 39431 presented at the 1998

SPE International Formation Damage Symposium, Lafayette, Louisiana, 18-19 February.

Kamenov, A. N. 2013. The Effect of Proppant Size and Concentration on Hydraulic Fracture Conductivity in Shale Reservoirs. MS thesis, Texas A&M University, College Station, Texas (May 2013).

Kmusser. A map of the Tarim River drainage basin. Digital Chart of the World and GTOPO data, labels based on GEOnet (December 2008).

[https://en.wikipedia.org/wiki/Tarim\\_Basin#/media/File:Tarimrivermap.png](https://en.wikipedia.org/wiki/Tarim_Basin#/media/File:Tarimrivermap.png)

Malagon, C., Pournik, M., and Hill, A.D. The Texture of Acidized Fracture Surfaces- Implications for Acid Fracture Conductivity. Paper SPE 102167-MS presented at the 2006 SPE Annual Technical Conference and Exhibition, San Antonio, Texas, 24-27 September.

Melendez, M.G. 2007b. The Effects of Acid Contact Time and Rock Surfaces on Acid Fracture Conductivity. MS thesis, Texas A&M University, College Station, Texas (August 2007).

Meyer, B.R., Bazan, L. W., Jacot, R.H., and Lattibeaudiere, M. G. Optimization of Multiple Tansverse Hydraulic Fracture in Horizontal Wellbore. SPE Paper 13732, 2010.

Mou, J. 2009. Modeling Acid Transport and Non-Uniform Etching in a Stochastic Domain in Acid Fracturing. Ph.D. dissertation, College Station: Texas A&M University.



- Mukherjee, H., and Economides, M.J. A Parametric Comparison of Horizontal and Vertical Well Performance. SPE Paper 18303,1991.
- Navarrete, R.C., Miller, M.J., and Gordon, J.E. Laboratory and Theoretical Studies for Acid Fracture Stimulation Optimization. Paper SPE 39776 presented at the 1998 SPE Permian Basin Oil and Gas Recovery Conference, Midland, Texas, 23-26 March.
- Neumann, L. F., Oliveira, T. J. L., and Fernandes, P. D. 2012. Building Acid Frac Conductivity in Highly-Confined Carbonates. Paper SPE 152164 presented at the SPE Hydraulic Fracturing Technology Conference, The Woodlands, Texas, 6-8 February
- Neumann, L. F., de Oliveira e Sousa, J. L. A. O., and Oliveira, T. J. L. 2012. Acid Fracturing: New Insights on Acid Etching Patterns from Experimental Investigation. Paper SPE 152179 presented at the SPE Hydraulic Fracturing Technology Conference, The Woodlands, Texas, 6-8 February
- Nierode, D. E., and K. F. Kruk. An Evaluation of Acid Fluid Loss Additives Retarded Acids, and Acidized Fracture Conductivity. In Fall Meeting of the Society of Petroleum Engineers of AIME, 1973.
- Oeth, C.V. Three-Dimensional Modeling of Acid Transport and Etching In A Fracture. Ph.D. dissertation, College Station: Texas A&M University. College Station, Texas (2013).
- Pournik, M., Zou, C., Malagon Nieto, C., Melendez, M. G., Zhu, D., Hill, A.D. and Weng, X. 2007. Small-Scale Fracture Conductivity Created by Modern Acid-

Fracture Fluids. Paper SPE 106272 presented at the SPE Hydraulic Fracturing Technology Conference, College Station, Texas, U.S.A, 29-31 January.

Wei, Y., and Economides, M.J., Transverse Hydraulic Fracture from a Horizontal Well, SPE Paper 94671, 2005.

Zou, C.L. Development and Testing of an Advanced Acid Fracture Conductivity Apparatus. M.S. Thesis, Texas A&M University, College Station, Texas (2005)

APPENDIX A

WELL 1 CONDUCTIVITY CALCULATION SHEET

**Table A-1.** Unpropried fracture conductivity test results on well 1 sample A

**Data used for calculations**

Length of fracture over pressure drop (	5.25
Width of fracture face (in) =	1.75
RMM of nitrogen (kg / mole) =	0.028
Compressibility factor, Z =	1.00
R (J / mol K) =	8.3144
Temperature, T (K) =	293.15
Viscosity of nitrogen (Pa.s) =	1.75923E-05
Density of nitrogen (kg/m <sup>3</sup> ) =	1.16085
Standard pressure (psi) =	14.7
Overburden ram area (in <sup>2</sup> ) =	125
Rock surface area (in <sup>2</sup> ) =	10.00

**Calibration Data**

Pcell =	0	psi
ΔP Front =		psi
Load from Frame (psi) =	0.00	psi
Proppant wieght		gm
Fracture Surface Area	10.00	sq in
Proppant Conc in the fracture	0.000	lb/sq ft

**Calculations**

Time (hrs)	Overburden Pressure	Flow Rate	P <sub>Cell</sub>	ΔP	y-axis, (P <sub>1</sub> <sup>2</sup> -P <sub>2</sub> <sup>2</sup> )M/ (2ZRTL)	x-axis, ρqμ/h	slope from Graph	k <sub>f</sub> -w
(hrs)	(psi)	(slm)	(psi)	(psi)	(1/m <sup>3</sup> )	no unit		(md-ft)
	500	1.0000	50.0600	0.1800	4.78E+04	7.66E-09	7.80E+12	426.45
		0.8000	50.2000	0.1300	3.46E+04	6.13E-09		
		0.5700	50.1800	0.0800	2.13E+04	4.36E-09		
		0.3800	50.0300	0.0400	1.06E+04	2.91E-09		
	1000	0.2000	50.0700	0.1200	3.18E+04	1.53E-09	4.68E+13	71.11
		0.3900	50.0500	0.3100	8.22E+04	2.99E-09		
		0.5700	50.0700	0.5700	1.51E+05	4.36E-09		
		0.7200	50.0600	0.8200	2.18E+05	5.51E-09		
	2000	0.1000	49.9500	0.4600	1.22E+05	7.66E-10	2.99E+14	11.11
		0.2100	50.0600	1.2800	3.40E+05	1.61E-09		
		0.2900	50.0800	1.9900	5.28E+05	2.22E-09		
		0.3600	50.0300	2.7200	7.21E+05	2.76E-09		

**Table A-2. Propped fracture conductivity test results on well 1 sample A**

**Data used for calculations**

Length of fracture over pressure drop (	5.25
Width of fracture face (in) =	1.75
RMM of nitrogen (kg / mole) =	0.028
Compressibility factor, Z =	1.00
R (J / mol K) =	8.3144
Temperature, T (K) =	293.15
Viscosity of nitrogen (Pa .s ) =	1.75923E-05
Density of nitrogen (kg/m <sup>3</sup> ) =	1.16085
Standard pressure (psi) =	14.7
Overburden ram area (in <sup>2</sup> ) =	125
Rock surface area (in <sup>2</sup> ) =	10.00

**Calibration Data**

Pcell =	0	psi
ΔP Front =		psi
Load from Frame (psi) =	0.00	psi
Proppant weight		gm
Fracture Surface Area	10.00	sq in
Proppant Conc in the fracture	0.000	lb/sq ft

**Calculations**

Time (hrs)	Overburden Pressure	Flow Rate	P <sub>Cell</sub>	ΔP	y-axis, (P <sub>1</sub> <sup>2</sup> -P <sub>2</sub> <sup>2</sup> )M/ (2ZRTL)	x-axis, ρqμ/h	slope from Graph	k <sub>r</sub> -W
(hrs)	(psi)	(slm)	(psi)	(psi)	(1/m <sup>3</sup> )	no unit		(md-ft)
	500	2.8500	50.4300	0.0136	3.63E+03	2.18E-08	1.40E+11	<b>23796.33</b>
		5.4600	50.6000	0.0226	6.04E+03	4.18E-08		
		7.5900	50.3800	0.0318	8.48E+03	5.81E-08		
		9.4800	50.5900	0.0400	1.07E+04	7.26E-08		
	1000	3.7400	50.0900	0.0150	3.98E+03	2.86E-08	1.82E+11	<b>18244.40</b>
		5.4700	50.1700	0.0280	7.44E+03	4.19E-08		
		7.7700	50.1600	0.0380	1.01E+04	5.95E-08		
		9.5000	50.2400	0.0460	1.22E+04	7.27E-08		
	3000	3.7500	50.0800	0.0450	1.19E+04	2.87E-08	1.62E+12	<b>2055.79</b>
		5.4700	50.1000	0.1100	2.92E+04	4.19E-08		
		7.4000	50.1650	0.2000	5.32E+04	5.67E-08		
		8.2000	50.0800	0.2560	6.79E+04	6.28E-08		
	5000	1.4200	50.0300	0.0330	8.75E+03	1.09E-08	2.36E+12	<b>1410.83</b>
		2.7500	50.1000	0.1200	3.19E+04	2.11E-08		
		3.6700	50.1800	0.1800	4.78E+04	2.81E-08		
		4.7500	50.1700	0.2600	6.91E+04	3.64E-08		
	7000	0.7700	50.1500	0.0400	1.06E+04	5.90E-09	4.25E+12	<b>782.85</b>
		1.3200	50.0000	0.0900	2.39E+04	1.01E-08		
		2.4400	50.1100	0.2400	6.37E+04	1.87E-08		
		1.9500	50.0500	0.1800	4.78E+04	1.49E-08		

**Table A-3. Acid fracture conductivity test results on well 1 sample A**

**Data used for calculations**

Length of fracture over pressure drop (	5.25
Width of fracture face (in) =	1.75
RMM of nitrogen (kg / mole) =	0.028
Compressibility factor, Z =	1.00
R (J / mol K) =	8.3144
Temperature, T (K) =	293.15
Viscosity of nitrogen (Pa .s ) =	1.75923E-05
Density of nitrogen (kg/m <sup>3</sup> ) =	1.16085
Standard pressure (psi) =	14.7
Overburden ram area (in <sup>2</sup> ) =	125
Rock surface area (in <sup>2</sup> ) =	10.00

**Calibration Data**

Pcell =	0	psi
ΔP Front =		psi
Load from Frame (psi) =	0.00	psi
Proppant weight		gm
Fracture Surface Area	10.00	sq in
Proppant Conc in the fracture	0.000	lb/sq ft

<b>Polymer Loading</b>	lbm/Mgal
<b>Gas Rate</b>	slm
<b>Proppant loading</b>	ppa
<b>Breaker</b>	

**Calculations**

Time (hrs)	Overburden Pressure (psi)	Flow Rate (slm)	P <sub>Cell</sub> (psi)	ΔP (psi)	y-axis, (P <sub>1</sub> <sup>2</sup> -P <sub>2</sub> <sup>2</sup> )M/(2ZRTL) (1/m <sup>3</sup> )	x-axis, ρqu/h (no unit)	slope from Graph	k <sub>r-w</sub> (md-ft)
500	500	0.9230	50.4400	0.0500	1.33E+04	7.07E-09	3.40E+12	976.43
		1.5920	50.2800	0.1100	2.93E+04	1.22E-08		
		2.1530	50.2650	0.1600	4.26E+04	1.65E-08		
		2.7370	50.2000	0.2300	6.12E+04	2.10E-08		
1000	1000	0.9080	50.0000	0.1500	3.98E+04	6.95E-09	9.67E+12	343.66
		1.5060	50.0000	0.2900	7.69E+04	1.15E-08		
		2.1290	50.0600	0.4700	1.25E+05	1.63E-08		
		2.5920	50.0100	0.6200	1.64E+05	1.98E-08		
1500	1500	0.7700	50.0000	0.2500	6.63E+04	5.90E-09	1.87E+13	178.12
		1.3500	50.0000	0.5300	1.40E+05	1.03E-08		
		1.6100	50.0000	0.6900	1.83E+05	1.23E-08		
		1.8400	50.0000	0.8300	2.20E+05	1.41E-08		
2000	2000	0.4200	50.0800	0.1800	4.78E+04	3.22E-09	2.24E+13	148.30
		0.8000	50.0600	0.4200	1.11E+05	6.13E-09		
		0.9100	50.0200	0.5000	1.33E+05	6.97E-09		
		0.7100	50.0600	0.3700	9.82E+04	5.44E-09		
2000	2000	0.4200	50.0400	0.2200	5.84E+04	3.22E-09	3.20E+13	103.96
		0.8000	50.2800	0.5800	1.54E+05	6.13E-09		
		0.9300	50.0200	0.6900	1.83E+05	7.12E-09		
		0.6800	50.0500	0.4900	1.30E+05	5.21E-09		
3000	3000	0.2000	50.0400	0.1300	3.45E+04	1.53E-09	4.42E+13	75.30
		0.5500	50.0900	0.4600	1.22E+05	4.21E-09		
		0.8500	50.0300	0.9100	2.41E+05	6.51E-09		
		1.0800	49.9900	1.2400	3.29E+05	8.27E-09		
4000	4000	0.2100	50.0800	0.2200	5.84E+04	1.61E-09	5.95E+13	55.88
		0.5000	50.0200	0.6100	1.62E+05	3.83E-09		
		0.8100	50.0700	1.2400	3.29E+05	6.20E-09		
		0.6700	50.0000	0.9900	2.62E+05	5.13E-09		
5000	5000	0.1640	50.0800	0.1800	4.78E+04	1.26E-09	7.17E+13	46.37
		0.3100	50.0400	0.4100	1.09E+05	2.37E-09		
		0.5500	50.0000	0.9000	2.39E+05	4.21E-09		
		0.7000	50.1500	1.2900	3.43E+05	5.36E-09		
6000	6000	0.1200	50.3000	0.2200	5.86E+04	9.19E-10	1.02E+14	32.49
		0.3100	50.3800	0.6200	1.65E+05	2.37E-09		
		0.5900	50.3800	1.4800	3.95E+05	4.52E-09		
		0.6900	50.3300	1.9000	5.06E+05	5.28E-09		
7000	7000	0.1200	50.1200	0.2800	7.44E+04	9.19E-10	1.39E+14	23.90
		0.3100	50.2400	0.8400	2.24E+05	2.37E-09		
		0.5900	50.2800	2.0200	5.38E+05	4.52E-09		
		0.7000	50.1300	2.6000	6.91E+05	5.36E-09		

## APPENDIX B

### WELL 2 CONDUCTIVITY CALCULATION SHEET

**Table B-1.** Unpropped fracture conductivity test results on well 2 sample B

**Data used for calculations**

Length of fracture over pressure drop (	5.25
Width of fracture face (in) =	1.75
RMM of nitrogen (kg / mole) =	0.028
Compressibility factor, Z =	1.00
R (J / mol K) =	8.3144
Temperature, T (K) =	293.15
Viscosity of nitrogen (Pa .s) =	1.75923E-05
Density of nitrogen (kg/m <sup>3</sup> ) =	1.16085
Standard pressure (psi) =	14.7
Overburden ram area (in <sup>2</sup> ) =	125
Rock surface area (in <sup>2</sup> ) =	10.00

**Calibration Data**

Pcell =	0	psi
ΔP Front =		psi
Load from Frame (psi) =	0.00	psi
Proppant weight		gm
Fracture Surface Area	10.00	sq in
Proppant Conc in the fracture	0.000	lb/sq ft

**Calculations**

Time (hrs)	Overburden Pressure (psi)	Flow Rate (slm)	P <sub>cell</sub> (psi)	ΔP (psi)	y-axis, (P <sub>1</sub> <sup>2</sup> -P <sub>2</sub> <sup>2</sup> )/ (2ZRTL) (1/m <sup>3</sup> )	x-axis, ρqμ/h (no unit)	slope from Graph	k <sub>f</sub> -w (md-ft)
Unpropped	500	0.3600	49.5100	0.6000	1.58E+05	2.76E-09	7.93E+13	41.90
		0.5800	49.5100	1.2600	3.31E+05	4.44E-09		
		0.7300	49.5500	1.5100	3.98E+05	5.59E-09		
		0.8500	49.5300	1.7400	4.58E+05	6.51E-09		
					0.00E+00	0.00E+00		
	1000	0.1100	49.5400	0.8900	2.34E+05	8.42E-10	1.80E+14	18.42
		0.2000	49.5700	1.3300	3.50E+05	1.53E-09		
		0.2900	49.5400	1.7800	4.69E+05	2.22E-09		
		0.4300	49.5300	2.5700	6.76E+05	3.29E-09		
					0.00E+00	0.00E+00		
	2000	0.0900	49.5800	2.1300	5.61E+05	6.89E-10	7.81E+14	4.26
		0.1300	49.5700	2.9800	7.85E+05	9.95E-10		
		0.1700	49.5800	4.0400	1.06E+06	1.30E-09		
		0.2200	49.5700	5.0400	1.33E+06	1.68E-09		
					0.00E+00	0.00E+00		
	3000	0.0200	49.4400	1.8700	4.91E+05	1.53E-10	1.22E+15	2.73
		0.0400	49.4400	2.4500	6.44E+05	3.06E-10		
		0.0600	49.3900	3.2700	8.59E+05	4.59E-10		
		0.0900	49.4100	4.3200	1.13E+06	6.89E-10		
					0.00E+00	0.00E+00		
	4000	0.0100	49.4500	2.9200	7.67E+05	7.66E-11	2.56E+15	1.30
		0.0200	49.4500	3.5000	9.20E+05	1.53E-10		
		0.0300	49.4800	4.5800	1.20E+06	2.30E-10		
		0.0400	49.4600	5.0400	1.32E+06	3.06E-10		
					0.00E+00	0.00E+00		

**Table B-2. Propped fracture conductivity test results on well 2 sample B**

**Data used for calculations**

Length of fracture over pressure drop (	5.25
Width of fracture face (in) =	1.75
RMM of nitrogen (kg / mole) =	0.028
Compressibility factor, Z =	1.00
R (J / mol K) =	8.3144
Temperature, T (K) =	293.15
Viscosity of nitrogen (Pa .s) =	1.75923E-05
Density of nitrogen (kg/m <sup>3</sup> ) =	1.16085
Standard pressure (psi) =	14.7
Overburden ram area (in <sup>2</sup> ) =	125
Rock surface area (in <sup>2</sup> ) =	10.00

**Calibration Data**

Pcell =	0	psi
ΔP Front =		psi
Load from Frame (psi) =	0.00	psi
Proppant wieght		gram
Fracture Surface Area	10.00	sq in
Proppant Conc in the fracture	0.000	lb/sq ft

**Calculations**

Time (hrs)	Overburden Pressure	Flow Rate	P <sub>Cell</sub>	ΔP	y-axis, (P <sub>1</sub> <sup>2</sup> -P <sub>2</sub> <sup>2</sup> )M/ (2ZRTL)	x-axis, pqw/h	slope from Graph	k <sub>f</sub> -W
(hrs)	(psi)	(slm)	(psi)	(psi)	(1/m <sup>3</sup> )	no unit		(md-ft)
	2000	3.20	50.24	0.67	1.78E+05	2.45E-08	2.95E+11	<b>11254.76</b>
		5.50	50.28	0.68	1.81E+05	4.21E-08		
		6.87	50.23	0.70	1.86E+05	5.26E-08		
		5.73	50.28	0.70	1.86E+05	4.39E-08		
	3000	2.77	50.25	0.67	1.78E+05	2.12E-08	7.16E+11	<b>4641.35</b>
		3.93	50.26	0.69	1.84E+05	3.01E-08		
		4.82	50.23	0.70	1.86E+05	3.69E-08		
		5.83	50.27	0.72	1.92E+05	4.46E-08		
		6.91	50.21	0.76	2.02E+05	5.29E-08		
	4000	2.83	50.18	0.70	1.86E+05	2.17E-08	1.51E+12	<b>2196.54</b>
		3.85	50.18	0.72	1.91E+05	2.95E-08		
		4.79	50.17	0.76	2.02E+05	3.67E-08		
		5.87	50.20	0.82	2.18E+05	4.49E-08		
		6.86	50.13	0.87	2.31E+05	5.25E-08		
	5000	3.10	50.12	0.78	2.07E+05	2.37E-08	3.70E+12	<b>898.54</b>
		4.89	50.14	0.91	2.42E+05	3.74E-08		
		5.87	50.14	1.03	2.74E+05	4.49E-08		
		6.88	50.17	1.19	3.16E+05	5.27E-08		
	7000	2.96	50.13	1.09	2.90E+05	2.27E-08	1.30E+13	<b>255.73</b>
		5.07	50.19	1.70	4.52E+05	3.88E-08		
		5.85	50.15	2.07	5.50E+05	4.48E-08		
		6.80	50.15	2.56	6.80E+05	5.21E-08		

**Table B-3. Acid fracture conductivity test results on well 2 sample B**

**Data used for calculations**

Length of fracture over pressure drop (	5.25
Width of fracture face (in) =	1.75
RMM of nitrogen (kg / mole) =	0.028
Compressibility factor, Z =	1.00
R (J / mol K) =	8.3144
Temperature, T (K) =	293.15
Viscosity of nitrogen (Pa .s) =	1.75923E-05
Density of nitrogen (kg/m <sup>3</sup> ) =	1.16085
Standard pressure (psi) =	14.7
Overburden ram area (in <sup>2</sup> ) =	125
Rock surface area (in <sup>2</sup> ) =	10.00

**Calibration Data**

Pcell =	0	psi
ΔP Front =		psi
Load from Frame (psi) =	0.00	psi
Proppant weight		gm
Fracture Surface Area	10.00	sq in
Proppant Conc in the fracture	0.000	lb/sq ft

**Calculations**

Time (hrs)	Overburden Pressure	Flow Rate	P <sub>cell</sub>	ΔP	y-axis, (P <sub>1</sub> <sup>2</sup> -P <sub>2</sub> <sup>2</sup> )M/ (2ZRTL)	x-axis, ρqm/h	slope from Graph	k <sub>r-w</sub>
(hrs)	(psi)	(slm)	(psi)	(psi)	(1/m <sup>3</sup> )	no unit		(md-ft)
T04 Acid Fracturte	500	0.20	50.03	0.01	1.33E+03	1.52E-09	1.63E+11	20341.84
		1.08	50.03	0.01	2.65E+03	8.25E-09		
		2.11	50.04	0.01	2.65E+03	1.61E-08		
		3.01	50.05	0.02	5.31E+03	2.30E-08		
	1000	1.22	50.05	0.01	3.77E+03	9.31E-09	7.08E+11	4697.38
		2.03	50.03	0.03	6.98E+03	1.56E-08		
		3.04	50.04	0.05	1.29E+04	2.33E-08		
		4.02	50.08	0.07	1.88E+04	3.08E-08		
	2000	2.06	50.03	0.07	1.93E+04	1.58E-08	2.01E+12	1655.54
		3.06	50.02	0.12	3.21E+04	2.35E-08		
		4.10	50.04	0.18	4.66E+04	3.14E-08		
		5.06	50.02	0.25	6.59E+04	3.87E-08		
	3000	2.08	50.07	0.19	4.93E+04	1.59E-08	5.31E+12	626.09
		3.05	50.08	0.31	8.25E+04	2.34E-08		
		4.11	50.06	0.46	1.22E+05	3.14E-08		
		5.05	50.08	0.65	1.72E+05	3.87E-08		
	4000	1.99	50.08	0.26	6.81E+04	1.52E-08	9.81E+12	338.73
		2.99	50.09	0.49	1.31E+05	2.29E-08		
		4.06	50.05	0.77	2.05E+05	3.11E-08		
		5.00	50.07	1.12	2.97E+05	3.83E-08		
	5000	2.06	50.08	0.56	1.49E+05	1.57E-08	1.75E+13	190.21
		3.03	50.07	0.97	2.57E+05	2.32E-08		
		4.07	50.07	1.45	3.84E+05	3.12E-08		
		5.03	50.05	2.08	5.51E+05	3.85E-08		
	6000	0.98	50.05	0.42	1.10E+05	7.52E-09	2.93E+13	113.41
		2.00	50.06	1.00	2.65E+05	1.53E-08		
		3.03	50.07	1.78	4.72E+05	2.32E-08		
		4.02	50.05	2.61				
		5.01	50.07	3.78	1.00E+06	3.84E-08		
	7000	1.04	50.06	0.70	1.87E+05	7.93E-09	4.64E+13	71.59
		2.03	50.05	1.65	4.37E+05	1.56E-08		
		3.01	50.08	2.84	7.53E+05	2.30E-08		
		4.00	50.07	4.15				
		4.98	50.08	5.92	1.57E+06	3.82E-08		



**Table B-4.** Unropped fracture conductivity test results on well 2 sample C

**Data used for calculations**

Length of fracture over pressure drop (	5.25
Width of fracture face (in) =	1.65
RMM of nitrogen (kg / mole) =	0.028
Compressibility factor, Z =	1.00
R (J / mol K) =	8.3144
Temperature, T (K) =	293.15
Viscosity of nitrogen (Pa .s) =	1.75923E-05
Density of nitrogen (kg/m <sup>3</sup> ) =	1.16085
Standard pressure (psi) =	14.7
Overburden ram area (in <sup>2</sup> ) =	125
Rock surface area (in <sup>2</sup> ) =	10.00

**Calibration Data**

Pcell =	0.6	psi
ΔP Front =	0	psi
Load from Frame (psi) =	0.00	psi
Proppant wieght		gram
Fracture Surface Area	10.00	sq in
Proppant Conc in the fracture	0.000	lb/sq ft

**Polymer Loading**

lbm/Mgal

**Gas Rate**

slm

**Proppant loading**

ppa

**Breaker**

**Calculations**

Time (hrs)	Overburden Pressure (psi)	Flow Rate (slm)	P <sub>Cell</sub> (psi)	ΔP (psi)	y-axis, (P <sub>1</sub> <sup>2</sup> -P <sub>2</sub> <sup>2</sup> )M/ (2ZRTL) (1/m <sup>3</sup> )	x-axis, ρqμ/h no unit	slope from Graph	k <sub>r-w</sub> (md-ft)
T13 Unropped	500	0.1520	50.0000	0.0400	1.05E+04	1.23E-09	6.22E+12	534.12
		0.3190	50.0000	0.0700	1.84E+04	2.59E-09		
		0.4750	50.0000	0.1000	2.63E+04	3.86E-09		
		0.6190	50.0000	0.1300	3.41E+04	5.03E-09		
	1000	0.1180	50.0000	0.0600	1.58E+04	9.58E-10	1.87E+13	177.70
		0.2760	50.0000	0.1400	3.68E+04	2.24E-09		
		0.4780	50.0000	0.2600	6.83E+04	3.88E-09		
		0.6210	50.0000	0.3500	9.19E+04	5.04E-09		
	2000	0.0690	50.0000	0.1200	3.15E+04	5.60E-10	7.20E+13	46.16
		0.2620	50.0000	0.5100	1.34E+05	2.13E-09		
		0.4390	50.0000	0.9100	2.39E+05	3.57E-09		
		0.5660	50.0000	1.2300	3.23E+05	4.60E-09		
	3000	0.0920	50.0000	0.3400	8.93E+04	7.47E-10	1.61E+14	20.71
		0.2650	50.0000	1.1300	2.97E+05	2.15E-09		
		0.4080	50.0000	1.8200	4.78E+05	3.31E-09		
		0.5150	50.0000	2.4600	6.46E+05	4.18E-09		
	4000	0.1090	50.0000	0.7400	1.94E+05	8.85E-10	2.94E+14	11.31
		0.1640	50.0000	1.1600	3.05E+05	1.33E-09		
		0.2760	50.0000	2.1700	5.70E+05	2.24E-09		
		0.3730	50.0000	3.1300	8.22E+05	3.03E-09		

**Table B-5. Propped fracture conductivity test results on well 2 sample C**

**Data used for calculations**

Length of fracture over pressure drop (	5.25
Width of fracture face (in) =	1.65
RMM of nitrogen (kg / mole) =	0.028
Compressibility factor, Z =	1.00
R (J / mol K) =	8.3144
Temperature, T (K) =	293.15
Viscosity of nitrogen (Pa .s) =	1.75923E-05
Density of nitrogen (kg/m <sup>3</sup> ) =	1.16085
Standard pressure (psi) =	14.7
Overburden ram area (in <sup>2</sup> ) =	125
Rock surface area (in <sup>2</sup> ) =	10.00

**Calibration Data**

Pcell =	0.6	psi
ΔP Front =	0	psi
Load from Frame (psi) =	0.00	psi
Proppant weight		gm
Fracture Surface Area	10.00	sq in
Proppant Conc in the fracture	0.000	lb/sq ft

**Calculations**

Time (hrs)	Overburden Pressure (psi)	Flow Rate (slm)	P <sub>Cell</sub> (psi)	ΔP (psi)	y-axis, (P <sub>1</sub> <sup>2</sup> -P <sub>2</sub> <sup>2</sup> )M/ (2ZRTL) (1/m <sup>3</sup> )	x-axis, ρqμ/h no unit	slope from Graph	k <sub>r-w</sub> (md-ft)
	1000	3.1350	49.6000	0.0100	2.61E+03	2.55E-08	2.66E+11	<b>12480.49</b>
		4.7530	49.6000	0.0200	5.22E+03	3.86E-08		
		5.7210	49.6000	0.0300	7.83E+03	4.65E-08		
		6.7740	49.6000	0.0400	1.04E+04	5.50E-08		
					0.00E+00	0.00E+00		
	2000	1.0200	49.0000	0.0100	2.59E+03	8.28E-09	4.06E+11	<b>8179.34</b>
		2.6250	49.0000	0.0200	5.17E+03	2.13E-08		
		3.2080	49.0000	0.0400	1.03E+04	2.61E-08		
		4.2860	49.0000	0.0500	1.29E+04	3.48E-08		
					0.00E+00	0.00E+00		
	3000	0.9450	49.0000	0.0100	2.59E+03	7.67E-09	6.27E+11	<b>5306.09</b>
		1.6200	49.0000	0.0210	5.43E+03	1.32E-08		
		2.0460	49.0000	0.0300	7.76E+03	1.66E-08		
		2.4600	49.0000	0.0400	1.03E+04	2.00E-08		
					0.00E+00	0.00E+00		
	4000	0.7190	49.2000	0.0200	5.19E+03	5.84E-09	1.12E+12	<b>2972.48</b>
		1.0290	49.2000	0.0300	7.78E+03	8.36E-09		
		1.3710	49.2000	0.0400	1.04E+04	1.11E-08		
		1.5400	49.2000	0.0500	1.30E+04	1.25E-08		
					0.00E+00	0.00E+00		
	5000	0.5290	49.0000	0.0100	2.59E+03	4.30E-09	1.60E+12	<b>2071.56</b>
		0.6530	49.0000	0.0200	5.17E+03	5.30E-09		
		0.9150	49.0000	0.0300	7.76E+03	7.43E-09		
		1.0920	49.0000	0.0400	1.03E+04	8.87E-09		
	7000	0.3660	49.0000	0.0300	7.76E+03	2.97E-09	3.90E+12	<b>852.16</b>
		0.5710	49.0000	0.0500	1.29E+04	4.64E-09		
		0.6400	49.0000	0.0600	1.55E+04	5.20E-09		
		0.7690	49.0000	0.0800	2.07E+04	6.25E-09		

**Table B-6. Acid fracture conductivity test results on well 2 sample C**

**Data used for calculations**

Length of fracture over pressure drop (	5.25
Width of fracture face (in) =	1.65
RMM of nitrogen (kg / mole) =	0.028
Compressibility factor, Z =	1.00
R (J / mol K) =	8.3144
Temperature, T (K) =	293.15
Viscosity of nitrogen (Pa .s ) =	1.75923E-05
Density of nitrogen (kg/m <sup>3</sup> ) =	1.16085
Standard pressure (psi) =	14.7
Overburden ram area (in <sup>2</sup> ) =	125
Rock surface area (in <sup>2</sup> ) =	10.00

**Calibration Data**

Pcell =	1	psi
ΔP Front =	0	psi
Load from Frame (psi) =	0.00	psi
Proppant weight		gm
Fracture Surface Area	10.00	sq in
Proppant Conc in the fracture	0.000	lb/sq ft

**Calculations**

Time (hrs)	Overburden Pressure	Flow Rate	P <sub>Cell</sub>	ΔP	y-axis, (P <sub>1</sub> <sup>2</sup> -P <sub>2</sub> <sup>2</sup> )M/(2ZRTL)	x-axis, ρqμ/h	slope from Graph	k <sub>r-w</sub>
(hrs)	(psi)	(slm)	(psi)	(psi)	(1/m <sup>3</sup> )	no unit		(md-ft)
T15 Acid	500	1.10	50.00	0.01	2.61E+03	8.92E-09	4.63E+11	7182.54
		1.57	50.00	0.02	5.22E+03	1.27E-08		
		2.66	50.00	0.03	7.83E+03	2.16E-08		
		2.93	50.00	0.04	1.04E+04	2.38E-08		
	1000	0.4380	50.0000	0.0100	2.61E+03	3.56E-09	8.06E+11	4125.97
		0.5680	50.0000	0.0200	5.22E+03	4.61E-09		
		1.1460	50.0000	0.0300	7.83E+03	9.31E-09		
		1.9120	50.0000	0.0500	1.30E+04	1.55E-08		
	2000	0.2550	50.0000	0.0200	5.22E+03	2.07E-09	2.71E+12	1225.52
		0.5190	50.0000	0.0400	1.04E+04	4.21E-09		
		0.7550	50.0000	0.0600	1.57E+04	6.13E-09		
		0.9640	50.0000	0.0800	2.09E+04	7.83E-09		
	3000	0.2060	50.0000	0.0300	7.83E+03	1.67E-09	8.64E+12	384.93
		0.3190	50.0000	0.0600	1.57E+04	2.59E-09		
		0.3740	50.0000	0.0700	1.83E+04	3.04E-09		
		0.5780	50.0000	0.1300	3.39E+04	4.69E-09		
	4000	0.0090	50.0000	0.0400	1.04E+04	7.31E-11	1.26E+13	264.85
		0.2680	50.0000	0.1100	2.87E+04	2.18E-09		
		0.4120	50.0000	0.1900	4.96E+04	3.35E-09		
		0.4660	50.0000	0.2200	5.74E+04	3.78E-09		
	5000	0.1540	50.0000	0.0800	2.09E+04	1.25E-09	3.29E+13	101.16
		0.3430	50.0000	0.2600	6.79E+04	2.79E-09		
		0.4410	50.0000	0.3600	9.40E+04	3.58E-09		
		0.6030	50.0000	0.5400	1.41E+05	4.90E-09		
					0.00E+00	0.00E+00		
	7000	0.3010	50.0000	1.2100	3.16E+05	2.44E-09	1.95E+14	17.03
		0.3760	50.0000	1.6500	4.31E+05	3.05E-09		
		0.4670	50.0000	2.2100	5.77E+05	3.79E-09		
		0.5600	50.0000	2.7800	7.26E+05	4.55E-09		
					0.00E+00	0.00E+00		

APPENDIX C

WELL 3 CONDUCTIVITY CALCULATION SHEET

Table C-1. Unproped fracture conductivity test results on well 3 sample D

Data used for calculations

Length of fracture over pressure drop (ir	5.25
Width of fracture face (in) =	1.75
RMM of nitrogen (kg / mole) =	0.028
Compressibility factor, Z =	1.00
R (J / mol K) =	8.3144
Temperature, T (K) =	293.15
Viscosity of nitrogen (Pa .s) =	1.75923E-05
Density of nitrogen (kg/m <sup>3</sup> ) =	1.16085
Standard pressure (psi) =	14.7
Overburden ram area (in <sup>2</sup> ) =	125
Rock surface area (in <sup>2</sup> ) =	10.00

Calibration Data

Pcell =	0.4	psi
ΔP Front =	0.04	psi
Load from Frame (psi) =	0.00	psi
Proppant weight	3.2	gm
Fracture Surface Area	10.00	sq in
Proppant Conc in the fracture	0.101	lb/sq ft

Calculations

Time (hrs)	Overburden Pressure	Flow Rate	P <sub>Cell</sub>	ΔP	y-axis, (P <sub>1</sub> <sup>2</sup> -P <sub>2</sub> <sup>2</sup> )M/(2ZRTL)	x-axis, ρqm/h	slope from Graph	k <sub>r</sub> -w
(hrs)	(psi)	(slm)	(psi)	(psi)	(1/m <sup>3</sup> )	no unit		(md-ft)
T08 Unproped	500	3.29	50.07	0.01	-7.91E+03	2.52E-08	2.11E+11	15745.69
		5.13	50.15	0.02	-5.28E+03	3.92E-08		
		6.54	50.02	0.03	-2.64E+03	5.00E-08		
	1000	0.92	50.08	0.02	-5.28E+03	7.08E-09	7.21E+11	4610.99
		2.01	50.09	0.03	-2.64E+03	1.54E-08		
		2.93	50.05	0.05	2.64E+03	2.24E-08		
		3.98	50.03	0.08	1.05E+04	3.05E-08		
		4.9430	50.0400	0.1000	1.58E+04	3.79E-08		
	1000	2.3900	50.1000	0.0300	-2.64E+03	1.83E-08	8.10E+11	4104.18
		3.0030	50.1100	0.0500	2.64E+03	2.30E-08		
		3.9960	50.1000	0.0700	7.92E+03	3.06E-08		
		4.8720	50.1100	0.0900	1.32E+04	3.73E-08		
	2000	0.3910	50.3300	0.0200	-5.30E+03	2.99E-09	1.60E+12	2072.30
		1.7070	50.0600	0.0600	5.27E+03	1.31E-08		
		2.5450	50.0600	0.1000	1.58E+04	1.95E-08		
		3.5770	50.0600	0.1700	3.43E+04	2.74E-08		
	3000	0.9210	50.0600	0.0400	0.00E+00	7.05E-09	4.79E+12	693.90
		1.8640	50.0900	0.1500	2.90E+04	1.43E-08		
		2.4140	50.1100	0.2300	5.01E+04	1.85E-08		
		2.9870	50.1000	0.3300	7.65E+04	2.29E-08		
	4000	0.4960	50.0100	0.0600	5.27E+03	3.80E-09	1.04E+13	318.86
		0.8890	50.0100	0.1400	2.63E+04	6.81E-09		
		1.4020	50.0300	0.2900	6.59E+04	1.07E-08		
		1.9210	50.0200	0.4900	1.19E+05	1.47E-08		

**Table C-2. Propped fracture conductivity test results on well 3 sample D**

**Data used for calculations**

Length of fracture over pressure drop (lr)	5.25
Width of fracture face (in) =	1.75
RMM of nitrogen (kg / mole) =	0.028
Compressibility factor, Z =	1.00
R (J / mol K) =	8.3144
Temperature, T (K) =	293.15
Viscosity of nitrogen (Pa .s ) =	1.75923E-05
Density of nitrogen (kg/m <sup>3</sup> ) =	1.16085
Standard pressure (psi) =	14.7
Overburden ram area (in <sup>2</sup> ) =	125
Rock surface area (in <sup>2</sup> ) =	10.00

**Calibration Data**

Pcell =	0.4	psi
ΔP Front =	0.04	psi
Load from Frame (psi) =	0.00	psi
Proppant weight	3.2	gm
Fracture Surface Area	10.00	sq in
Proppant Conc in the fracture	0.101	lb/sq ft

**Calculations**

Time (hrs)	Overburden Pressure	Flow Rate	P <sub>Cell</sub>	ΔP	y-axis, (P <sub>1</sub> <sup>2</sup> -P <sub>2</sub> <sup>2</sup> )M/ (2ZRTL)	x-axis, ρqμ/h	slope from Graph	k <sub>r</sub> -w
(hrs)	(psi)	(slm)	(psi)	(psi)	(1/m <sup>3</sup> )	no unit		(md-ft)
T09 propped	500	3.9760	50.1700	0.0300	-2.64E+03	3.04E-08	3.15E+11	<b>10548.33</b>
		5.3780	50.0700	0.0400	0.00E+00	4.12E-08		
		6.5370	49.9000	0.0500	2.63E+03	5.01E-08		
		7.1080	49.6500	0.0600	5.24E+03	5.44E-08		
	1000	3.3670	49.1400	0.0200	-5.20E+03	2.58E-08	3.31E+11	<b>10057.56</b>
		4.4270	49.1600	0.0300	-2.60E+03	3.39E-08		
		5.5290	49.2000	0.0400	0.00E+00	4.23E-08		
		6.4170	49.2000	0.0500	2.60E+03	4.91E-08		
	2000	1.1975	49.1900	0.0400	0.00E+00	9.17E-09	1.42E+12	<b>2335.28</b>
		1.6680	49.1500	0.0600	5.20E+03	1.28E-08		
		2.4440	49.1200	0.0800	1.04E+04	1.87E-08		
		3.2620	49.1400	0.1300	2.34E+04	2.50E-08		
	3000	0.7540	49.1800	0.0300	-2.60E+03	5.77E-09	3.32E+12	<b>1000.91</b>
		1.1890	49.1400	0.0700	7.80E+03	9.10E-09		
		1.7350	49.1600	0.1200	2.08E+04	1.33E-08		
		2.2790	49.1800	0.1800	3.64E+04	1.75E-08		
	5000	0.3960	49.2800	0.0600	5.21E+03	3.03E-09	1.05E+13	<b>315.19</b>
		0.9280	49.2800	0.1800	3.65E+04	7.11E-09		
		1.4330	49.2800	0.3500	8.08E+04	1.10E-08		
		1.8530	49.2700	0.5100	1.22E+05	1.42E-08		
	7000	0.5100	49.2300	0.3400	7.81E+04	3.91E-09	4.64E+13	<b>71.66</b>
		0.7820	49.2300	0.6900	1.69E+05	5.99E-09		
		1.1360	49.2300	1.1500	2.89E+05	8.70E-09		
		1.3740	49.2300	1.5300	3.88E+05	1.05E-08		

**Table C-3. Acid fracture conductivity test results on well 3 sample D**

**Data used for calculations**

Length of fracture over pressure drop (ir	5.25
Width of fracture face (in) =	1.65
RMM of nitrogen (kg / mole) =	0.028
Compressibility factor, Z =	1.00
R (J / mol K) =	8.3144
Temperature, T (K) =	293.15
Viscosity of nitrogen (Pa . s) =	1.75923E-05
Density of nitrogen (kg/m <sup>3</sup> ) =	1.16085
Standard pressure (psi) =	14.7
Overburden ram area (in <sup>2</sup> ) =	125
Rock surface area (in <sup>2</sup> ) =	10.00

**Calibration Data**

Pcell =	1	psi
ΔP Front =	0.04	psi
Load from Frame (psi) =	0.00	psi
Proppant weight		gm
Fracture Surface Area		sq in
Proppant Conc in the fracture		lb/sq ft

**Calculations**

Time (hrs)	Overburden Pressure	Flow Rate	P <sub>Cell</sub>	ΔP	y-axis, (P <sub>1</sub> <sup>2</sup> -P <sub>2</sub> <sup>2</sup> )/M/ (2ZRTL)	x-axis, ρqμ/h	slope from Graph	k <sub>r-w</sub> (md-ft)
(hrs)	(psi)	(slm)	(psi)	(psi)	(1/m <sup>3</sup> )	no unit		
T10 Acid	500	0.3730	50.0000	0.0100	-7.83E+03	3.03E-09	1.30E+12	2548.62
		0.7000	50.0000	0.0200	-5.22E+03	5.68E-09		
		0.8390	50.0000	0.0300	-2.61E+03	6.81E-09		
		1.1310	50.0000	0.0400	0.00E+00	9.19E-09		
	1000	0.1200	50.2000	0.0100	-7.85E+03	9.75E-10	3.02E+12	1099.88
		0.2510	50.2000	0.0200	-5.24E+03	2.04E-09		
		0.3390	50.2000	0.0300	-2.62E+03	2.75E-09		
		0.4440	50.2000	0.0400	0.00E+00	3.61E-09		
	2000	0.0520	50.0000	0.0200	-5.22E+03	4.22E-10	2.22E+13	149.63
		0.1280	50.0000	0.0600	5.22E+03	1.04E-09		
		0.1790	50.0000	0.1000	1.57E+04	1.45E-09		
		0.2250	50.0000	0.1400	2.61E+04	1.83E-09		
	3000	0.0160	50.1000	0.0300	-2.61E+03	1.30E-10	7.73E+13	43.00
		0.0440	50.1000	0.0900	1.31E+04	3.57E-10		
		0.0760	50.1000	0.1700	3.40E+04	6.17E-10		
		0.1250	50.1000	0.2900	6.54E+04	1.02E-09		
	5000	0.0860	50.0000	0.4800	1.15E+05	6.98E-10	2.31E+14	14.40
		0.1670	50.0000	1.0700	2.69E+05	1.36E-09		
		0.2630	50.0000	1.7000	4.33E+05	2.14E-09		
		0.3590	50.0000	2.4600	6.32E+05	2.92E-09		
	7000	0.0750	50.0000	1.7400	4.44E+05	6.09E-10	9.69E+14	3.43
		0.0950	50.0000	2.3100	5.92E+05	7.72E-10		
		0.1180	50.0000	3.0100	7.75E+05	9.58E-10		
		0.1290	50.0000	3.3700	8.69E+05	1.05E-09		

**Table C-4.** Unproped fracture conductivity test results on well 3 sample E

**Data used for calculations**

Length of fracture over pressure drop (r	5.25
Width of fracture face (in) =	1.65
RMM of nitrogen (kg / mole) =	0.028
Compressibility factor, Z =	1.00
R (J / mol K) =	8.3144
Temperature, T (K) =	293.15
Viscosity of nitrogen (Pa . s ) =	1.75923E-05
Density of nitrogen (kg/m <sup>3</sup> ) =	1.16085
Standard pressure (psi) =	14.7
Overburden ram area (in <sup>2</sup> ) =	125
Rock surface area (in <sup>2</sup> ) =	10.00

**Calibration Data**

Pcell =	0	psi
ΔP Front =	0	psi
Load from Frame (psi) =	0.00	psi
Proppant weight	3.2	gm
Fracture Surface Area	10.00	sq in
Proppant Conc in the fracture	0.101	lb/sq ft

**Calculations**

Time (hrs)	Overburden Pressure	Flow Rate	P <sub>Cell</sub>	ΔP	y-axis, (P <sub>1</sub> <sup>2</sup> -P <sub>2</sub> <sup>2</sup> )M/ (2ZRTL)	x-axis, ρqμ/h	slope from Graph	k <sub>r</sub> -W
(hrs)	(psi)	(slm)	(psi)	(psi)	(1/m <sup>3</sup> )	no unit		(md-ft)
T11 Unproped	500	0.09	50.00	0.05	1.33E+04	7.63E-10	7.67E+13	43.34
		0.17	50.00	0.22	5.83E+04	1.36E-09		
		0.22	50.00	0.33	8.75E+04	1.75E-09		
		0.31	50.00	0.56	1.48E+05	2.53E-09		
	1000	0.06	50.00	3.17	8.40E+05	5.12E-10	6.86E+14	4.84
		0.10	50.00	3.44	9.12E+05	7.96E-10		
		0.14	50.00	3.80	1.01E+06	1.16E-09		
		0.18	50.00	4.13	1.09E+06	1.48E-09		
	2000				0.00E+00	0.00E+00	#DIV/0!	#DIV/0!
					0.00E+00	0.00E+00		
					0.00E+00	0.00E+00		
					0.00E+00	0.00E+00		

**Table C-5. Propped fracture conductivity test results on well 3 sample E**

**Data used for calculations**

Length of fracture over pressure drop (ir	5.25
Width of fracture face (in) =	1.65
RMM of nitrogen (kg / mole) =	0.028
Compressibility factor, Z =	1.00
R (J / mol K) =	8.3144
Temperature, T (K) =	293.15
Viscosity of nitrogen (Pa .s ) =	1.75923E-05
Density of nitrogen (kg/m <sup>3</sup> ) =	1.16085
Standard pressure (psi) =	14.7
Overburden ram area (in <sup>2</sup> ) =	125
Rock surface area (in <sup>2</sup> ) =	10.00

**Calibration Data**

Pcell =	0	psi
ΔP Front =	0	psi
Load from Frame (psi) =	0.00	psi
Proppant wieght	3.2	gm
Fracture Surface Area	10.00	sq in
Proppant Conc in the fracture	0.101	lb/sq ft

**Calculations**

Time (hrs)	Overburden Pressure	Flow Rate	P <sub>Cell</sub>	ΔP	y-axis, (P <sub>1</sub> <sup>2</sup> -P <sub>2</sub> <sup>2</sup> )M/ (2ZRTL)	x-axis, ρqμ/h	slope from Graph	k <sub>r-w</sub>
(hrs)	(psi)	(slm)	(psi)	(psi)	(1/m <sup>3</sup> )	no unit		(md-ft)
T12 propped	500	3.9960	50.1000	0.0100	2.65E+03	3.25E-08	2.22E+11	14963.77
		5.6360	50.1000	0.0200	5.31E+03	4.58E-08		
		6.9250	50.1000	0.0300	7.96E+03	5.62E-08		
	1000	2.6880	49.5000	0.0100	2.63E+03	2.18E-08	2.33E+11	14251.42
		3.9480	49.5000	0.0200	5.26E+03	3.21E-08		
		5.3080	49.5000	0.0300	7.89E+03	4.31E-08		
		6.8530	49.5000	0.0400	1.05E+04	5.57E-08		
	2000	1.1150	49.3000	0.0100	2.62E+03	9.06E-09	4.07E+11	8158.14
		2.1190	49.3000	0.0200	5.24E+03	1.72E-08		
		3.1180	49.3000	0.0300	7.87E+03	2.53E-08		
		4.2300	49.3000	0.0500	1.31E+04	3.44E-08		
	4000	1.0830	49.5000	0.0700	1.84E+04	8.80E-09	1.75E+12	1899.15
		2.0260	49.5000	0.0800	2.10E+04	1.65E-08		
		3.0380	49.5000	0.1400	3.68E+04	2.47E-08		
		4.1040	49.5000	0.2300	6.05E+04	3.33E-08		
	6000	0.3340	49.6000	0.2800	7.38E+04	2.71E-09	2.23E+13	149.39
		0.5630	49.6000	0.4000	1.05E+05	4.57E-09		
		0.8240	49.6000	0.6000	1.58E+05	6.69E-09		
		0.9840	49.6000	0.7200	1.90E+05	7.99E-09		
	7000	0.2270	49.5000	0.5500	1.45E+05	1.84E-09	4.84E+13	68.75
		0.5630	49.5000	0.9900	2.60E+05	4.57E-09		
		0.7210	49.5000	1.2300	3.24E+05	5.86E-09		
		0.9730	49.5000	1.6700	4.39E+05	7.90E-09		
				0.0000				



**Table C-6. Acid fracture conductivity test results on well 3 sample E**

**Data used for calculations**

Length of fracture over pressure drop (in)	5.25
Width of fracture face (in) =	1.65
RMM of nitrogen (kg / mole) =	0.028
Compressibility factor, Z =	1.00
R (J / mol K) =	8.3144
Temperature, T (K) =	293.15
Viscosity of nitrogen (Pa .s) =	1.75923E-05
Density of nitrogen (kg/m <sup>3</sup> ) =	1.16085
Standard pressure (psi) =	14.7
Overburden ram area (in <sup>2</sup> ) =	125
Rock surface area (in <sup>2</sup> ) =	10.00

**Calibration Data**

Pcell =	1	psi
ΔP Front =	0	psi
Load from Frame (psi) =	0.00	psi
Proppant weight		gm
Fracture Surface Area		sq in
Proppant Conc in the fracture		lb/sq ft

**Calculations**

Time (hrs)	Overburden Pressure	Flow Rate	P <sub>Cell</sub>	ΔP	y-axis, (P <sub>1</sub> <sup>2</sup> -P <sub>2</sub> <sup>2</sup> )M/(2ZRTL)	x-axis, ρqm/h	slope from Graph	k <sub>f</sub> -w
(hrs)	(psi)	(slm)	(psi)	(psi)	(1/m <sup>3</sup> )	no unit		(md-ft)
T13 Acid	500	0.1750	50.0000	0.0400	1.04E+04	1.42E-09	1.25E+13	266.49
		0.2830	50.0000	0.0800	2.09E+04	2.30E-09		
		0.4560	50.0000	0.1400	3.65E+04	3.70E-09		
		0.5800	50.0000	0.2000	5.22E+04	4.71E-09		
	1000	0.1400	50.0000	0.0900	2.35E+04	1.14E-09	2.83E+13	117.52
		0.2640	50.0000	0.1800	4.70E+04	2.14E-09		
		0.4460	50.0000	0.3400	8.87E+04	3.62E-09		
		0.5110	50.0000	0.4200	1.10E+05	4.15E-09		
	2000	0.0500	50.0000	0.0300	7.83E+03	4.06E-10	3.25E+13	102.20
		0.1340	50.0000	0.1000	2.61E+04	1.09E-09		
		0.2140	50.0000	0.1800	4.70E+04	1.74E-09		
		0.3690	50.0000	0.3500	9.13E+04	3.00E-09		
	3000	0.1000	50.0000	0.1500	3.91E+04	8.12E-10	5.95E+13	55.84
		0.1760	50.0000	0.2800	7.31E+04	1.43E-09		
		0.3100	50.0000	0.5300	1.38E+05	2.52E-09		
		0.4030	50.0000	0.7100	1.85E+05	3.27E-09		
	5000	0.0540	50.0000	0.1400	3.65E+04	4.39E-10	9.67E+13	34.39
		0.1770	50.0000	0.4800	1.25E+05	1.44E-09		
		0.2960	50.0000	0.8500	2.22E+05	2.40E-09		
		0.4210	50.0000	1.2400	3.24E+05	3.42E-09		
	7000	0.1730	50.1000	0.7000	1.83E+05	1.40E-09	1.50E+14	22.20
		0.3070	50.1000	1.3100	3.42E+05	2.49E-09		
		0.4810	50.1000	2.1100	5.52E+05	3.91E-09		
		0.6150	50.1000	2.7600	7.21E+05	4.99E-09		